INVESTIGATION OF BACTERIAL CELLULOSE AS A CARBON FIBER PRECURSOR AND ITS POTENTIAL FOR PIEZOELECTRIC ENERGY HARVESTING

A Thesis

Presented to the Faculty of the Graduate School

of Cornell University

in Partial Fulfillment of the Requirements for the Degree of

Master of Science

by

Jonas Buettner

August 2014

ABSTRACT

Bacterial cellulose was investigated regarding its suitability as a carbon fiber precursor as well as its potential in energy harvesting applications due to its inherent piezoelectric properties.

Graphitization of bacterial cellulose was found to be insufficient up to treatment temperatures of 2200 °C. The resulting structure without hot-stretching during the process is amorphous.

Piezoelectricity was confirmed in bacterial cellulose. BC cantilevers were induced to oscillate via an electrical field applied across the thickness of the cantilever.

Due to the random network structure of BC, methods for aligned growth were tested. Spatially confined growth on a patterned PDMS substrate resulted in aligned fiber threads.

BIOGRAPHICAL SKETCH

Jonas Buettner was born in Nürnberg, Germany on September 29, 1985. He received his Bachelor of Science in 2010 from Hamburg University of Technology. Most of his work has been on nanoscale and sustainable materials.

ACKNOWLEDGMENTS

I would like to thank my advisor, Prof. Anil N. Netravali. I am grateful for his support, frequent exchanges and encouragement throughout my studies. Thanks also goes to my lab mates. The good atmosphere and interesting conversations made it a joy to come to work.

Gratitude is owed to Prof. R. Bruce van Dover. Joining my committee late and on short notice his expertise and patience helped in finishing the project.

Furthermore I'd like to acknowledge Prof. Lal, Dr. Ardanuc as well as Prof. Craighead and Vivek P. Adiga for their help in doing some of the experimental work. My gratitude goes to Dana Johnson from Corning, Inc., Prof. Carty and Dr. Lee from Alfred University whose furnaces I was able to utilize thanks to their help.

This work was performed in part at the Cornell NanoScale Facility, a member of the National Nanotechnology Infrastructure Network, which is supported by the National Science Foundation (Grant ECCS-0335765) and also made use of the Cornell Center for Materials Research Shared Facilities which are supported through the NSF MRSEC program (DMR-1120296).

TABLE OF CONTENTS

LIST OF FIGURES

1 Bacterial cellulose

Cellulose is said to be the most abundant natural material on earth [1] or at least the most common polymer [2]. A major structural component of the cell walls in trees, plants and algae, it is also found in animals and synthesized by a variety of bacteria and fungi. In light of the ongoing efforts to decrease humanity's footprint on earth cellulose offers to be a readily available natural material that is fully sustainable and has excellent properties. The breadth of cellulose sources combined with a highly versatile hierarchical structure leads to a multitude of different microstructures and morphologies. In spite of being available from the beginning of mankind, to this day cellulose has not been fully understood in all its forms. The most common forms, however, show exceptional mechanical properties, high elasticity and good thermal stability. Moreover, the adaptable morphology and the possibility of chemical alterations allow tailoring its behavior to specific requirements and needs. Furthermore it is non-toxic, bio- and blood-compatible. It is no wonder then that cellulose is at the forefront in research of natural and sustainable materials to replace conventional ones, where possible and particular so as a natural replacement for petroleum based materials. Having been used as paper and clothing in various forms for several millennia it is now used and investigated to be used in a wide range of applications ranging from composites [3] to biomedical devices [4].

The specific form of cellulose of interest in this thesis is bacterial cellulose (BC), also

known as microbial cellulose or biocellulose. As the name suggests BC is a secretion product of some bacteria cultures. It was first reported in 1886 by Brown [5]. While investigating acid fermenting bacteria Brown noticed what was back then commonly known as the "vinegar plant" growing as a product of some of his bacteria cultures. Other researchers had encountered and investigated this "plant" before but were not able to draw convincing conclusions about its nature [6, 7, 8]. Due to its distinct form from other acetic bacteria, he isolated and specifically cultivated the plant producing bacteria. After chemical investigations he found the so called plant consisted of cellulose. Brown proposed to name this ferment *Bacterium xylinum*, a name which has basically been kept to this date. The bacterium is commonly known as Acetobacter xylinum these days, though the name was recently corrected to Gluconacetobacter xylinus [9, 10]. However, A. xylinum is also widely used in the literature. Probably the widest known application of bacterial cellulose is nata de coco, a dessert from the Philippines and many other Southeast Asian countries, which is gelled fermented coconut juice along with some sweetener. The gelling happens through the fermentation activities by Acetobacter xylinum resulting in BC growth [11]. Properties and potential applications of BC have only been researched extensively in the last two decades. Citations of papers about bacterial cellulose have been steadily increasing with a surge in recent years jumping from 327 between 2002 and 2007 to 1013 from 2007 to 2012 [12].

In this chapter the structure and synthesis of bacterial cellulose will be discussed followed by an investigation of its properties and concluded with an overview over existing and promising applications in today's world.

1.1 Structure

Even though, cellulose has been used for millennia and is known since nearly two centuries, it's structure is still not fully understood. Cellulose is employed in a multitude of natural

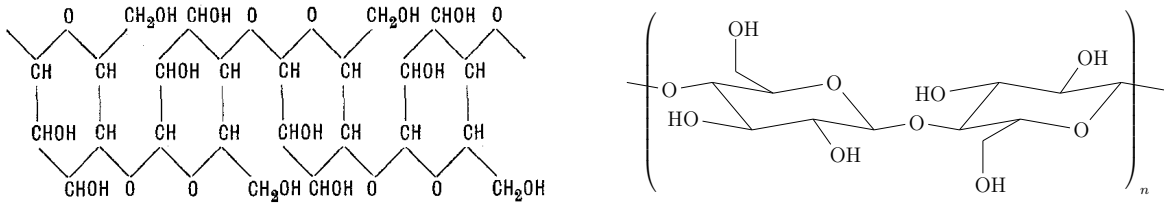

Figure 1.1: Cellulose structure as presented by Haworth [15] in 1928 on the left and a more contemporary representation of the repeating cellobiose unit. The degree of polymerisation (DP) of a cellulose chain is $2n$.

applications and, thus, its structure is highly adaptable showing alterations from source to source and even within one source. Pinpointing the exact nature of cellulose is, therefore, a difficult task and to this date refinements to the standard model are being made. Presented here is the most recent insight into cellulose structure.

Cellulose as a distinct material was first discovered in 1838 by Payen [13]. He extracted the major structural material from plants and woody matter and determined its chemical composition to be $C_6H_{10}O_5$. This material was then coined as *cellulose* in a review of Payen's publication in 1839 [14]. The chemical structure was first correctly predicted by Haworth [15] in 1928. It was known that cellulose consisted of cellobiose units, a dimer of β-D-glucopyranose monomers, that were linked together to form a longer molecule. Previous predictions had the correct ring structure based on the repeating glucose units but failed to link the individual components correctly. Figure 1.1 shows Haworth's correct proposal for the cellulose structure. The β-D-glucopyranose units are linked together with $(1 \longrightarrow 4)$ glycosidic bonds.

Advocating the idea of cellulose as a linear long-chain molecule of the newly discovered polymer materials since the early 1920s, Staudinger and Feuerstein [16] was able to prove his predictions in 1936 showing that it was indeed a linear macromolecule with degrees of polymerization of more than 2000. He also found that the length of the chain and with that the physical properties were highly dependent on the source and the extraction process

of the cellulose. Today it is known that the degree of polymerisation (DP) of cellulose molecules can reach up to 15 000 in cotton [17] and 16 000 in bacterial cellulose [18, 19]. However, it can also exist as shorter variants in wood, for example, having up to only 2000 units [2].

Cellulose exhibits a hierarchical morphology. About 30 cellulose macromolecules, in an oriented form, aggregate into elementary fibrils, several of which together form a so called microfibril. These are then arranged into the usually observed fibers [20].

In the elementary fibril configuration the chains have the ability to organise into a crystalline structure because of their highly oriented nature. In 1928, on the basis of Haworth's chemical structure, Meyer and Mark [21] proposed a corresponding crystal structure as shown in figure 1.3. Expanding on this proposal Peirce [22] suggested, in 1930, that cellulose is semicrystalline. In the microfibrils crystalline sections are broken up by amorphous regions. The degree of crystallinity, i.e. the volume fraction of crystalline parts, is highly dependent on the source and treatment process and like the degree of polymerization affects the properties [23]. The surface chains in the microfibrils are predicted to be in an unordered state whereas the inner chains are in crystalline form [1]. Thus, if more chains are bundled in a microfibril a higher degree of crystallinity in the overall structure is expected. Crystallinity differs from 40 % for plant cellulose up to 90 % for some algae variants [24]. The crystallinity of cellulose fiber is closely related to its mechanical properties and, hence, carries a significant importance. Bacterial cellulose has relatively high crystallinity which varies with environmental conditions but is generally determined to be around 75 % [25].

In addition to the hierarchical structure of the fibers, there is not one distinct crystal structure of cellulose but several polymorphs have been observed. Up to this point seven polymorphs are known. They are named cellulose I_α, I_β, II, III_I, III_{II}, IV_I and IV_{II} [1]. The principal polymorphs, i.e. cellulose I, II, III and IV, don't normally exist concurrently but

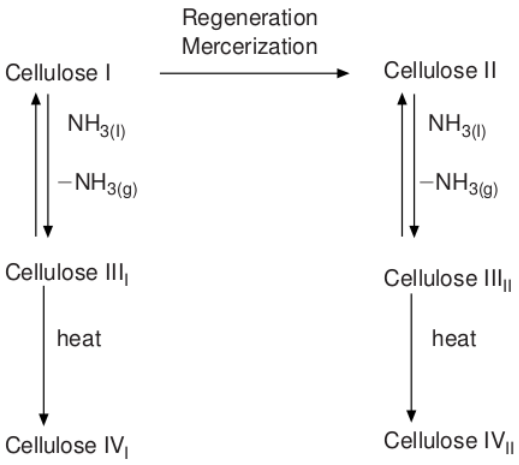

Figure 1.2: Cellulose polymorphs transformation diagram [1].

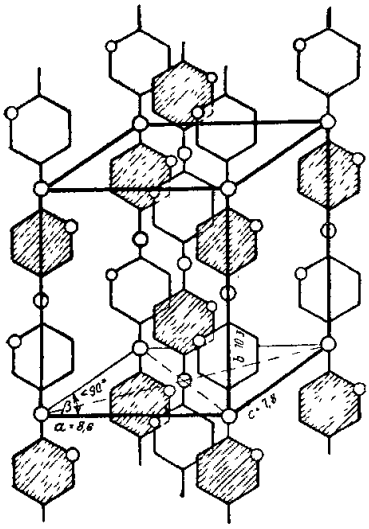

Figure 1.3: Cellulose crystal structure according to Meyer and Mark [21] in 1928.

can be transformed into each other as shown in figure 1.2.

Cellulose I and II are by far the most studied polymorphs and are usually employed in industrial applications such as apparel, composites, medical wound dressing and food packaging. Cellulose I, often referred to as native cellulose, is the polymorph that is found in plants and algae. Bacterial cellulose is of cellulose I type as well. Cellulose II, or regenerated and mercerized cellulose after the processes that yield this polymorph from cellulose I, is the thermodynamically stable form of cellulose. Regeneration and mercerization are irreversible processes during which the cellulose I material is dissolved and reprecipitated or swelled with sodium hydroxide, respectively, to form cellulose II. Due to the processes involved in cellulose extraction from plant matter, cellulose II generally has a lower degree of polymerization and crystallinity than native cellulose. The DP is usually around 250 to 500 and crystallinity is about 50 % [2]. The crystal structures of both allomorphs of cellulose I and cellulose II are compared in figure 1.4. The crystal structure of cellulose

II remains the same, no matter the original cellulose I type. Cellulose III is reversibly converted from either cellulose I or II via an ammonia treatment and with subsequent heating cellulose IV is formed. Cellulose III and IV are much less extensively studied than both I and II and thus there is much ambiguity about their structure and properties. They are not used in real world applications due to a decrease in mechanical properties [26]. A discussion of their structure will be omitted for these reasons.

The crystal structure proposed by Meyer and Mark [21] in 1928 for native cellulose was only deprecated by the findings of Atalla and Vanderhart [28] in 1984 using ^{13}C NMR. They originally found evidence that there exist two forms of cellulose I, termed cellulose I_α and I_β. Both allomorphs can coexist within the same microfibril, where the specific ratio usually depends on the source [26]. Plant cellulose mostly consists of I_β where I_α is more prevalent in cellulose produced by algae and bacteria. Cellulose I_α has a triclinic one chain unit cell whereas I_β has a $P2_1$ monoclinic two chain unit cell as shown in figure 1.4. Meyer's original crystal structure is similar to I_β which is consistent with the source used, ramie, which is rich in cellulose I_β . Bacterial cellulose has a high fraction of I_α estimated to be around 70 % [29].

Extraction and purification of cellulose from plant and wood matter is difficult without dissolving it to separate the cellulose from other components and subsequent regeneration. This is one of the main reasons why cellulose II is more widely spread in applications as compared to cellulose I. Cellulose II has a $P2_1$ monoclinic two-chain unit cell as shown in figure 1.4 The dimensions slightly depend on the conversion process, regeneration or mercerization, but a good approximation is given by $a = 8.10$ Å, $b = 9.04$ Å, $c = 10.36$ Å and $\gamma = 117.1°$. One distinguishing feature between cellulose I and II besides the different unit cell parameters is the configuration of the chains. Whereas in cellulose I the molecular chains lie in a parallel configuration [30], they are antiparallel in cellulose II [31]. The direction

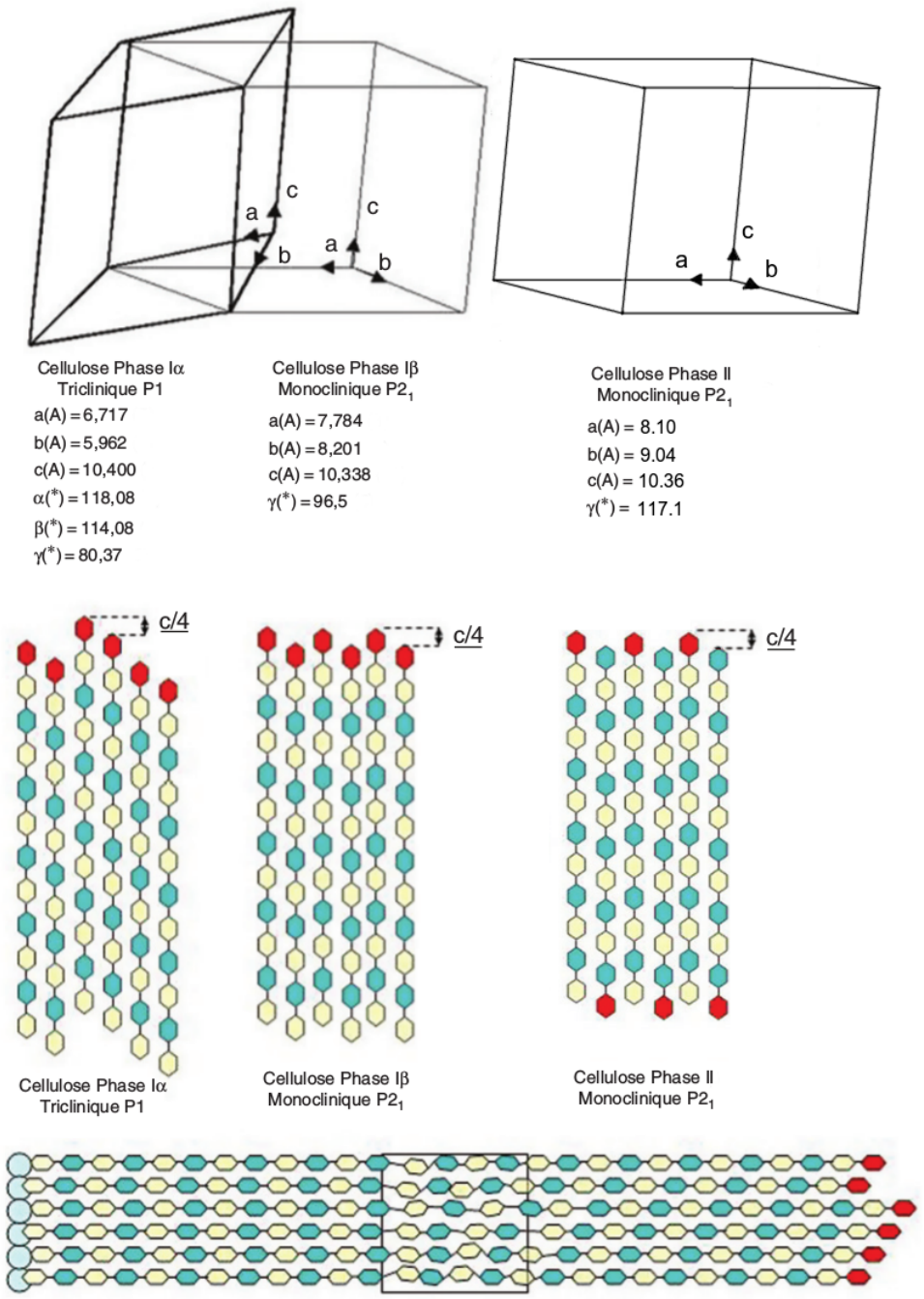

Figure 1.4: Schematic comparison of cellulose I_α , I_β and II unit cells including the chain stacking with parallel alignment for cellulose I and anti-parallel for celluose II. A schematic of the simultaneous existence of both cellulose I_α and I_β structures in a single fibril is shown at the bottom (adapted from [26]).

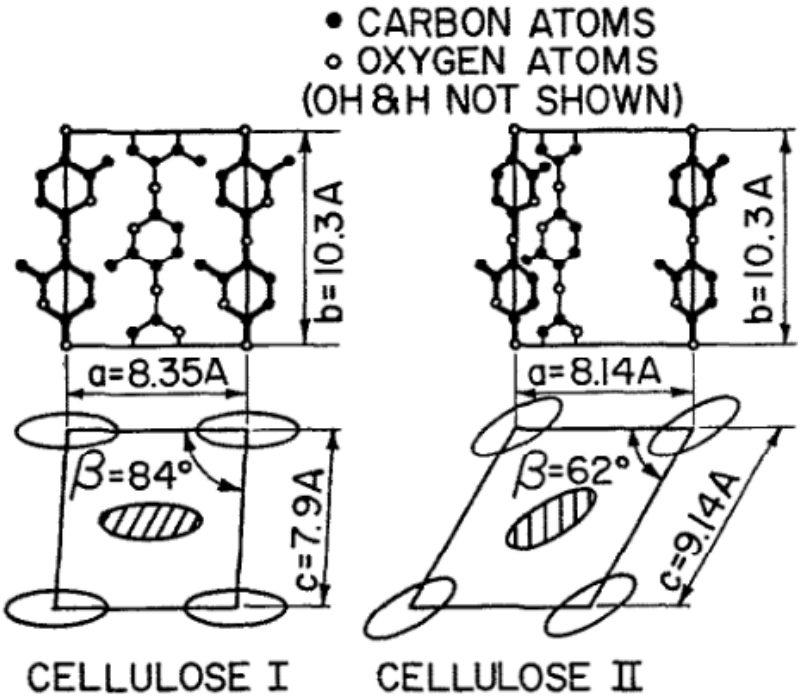

Figure 1.5: Graphical crystal structure comparison between cellulose I_β and cellulose II [27]. Compared to figure 1.4, here $\beta = 180° - \gamma$ and $\vec{b}$ is along the chain direction instead of $\vec{c}$.

for the chains for these definitions is set to be positive in the direction of the $(1 \longrightarrow 4)$ glycosidic bond. The chain configuration results in differences in the hydrogen-bonding between the chains.

Bacterial cellulose is highly crystalline cellulose I with a high I_α content and is very low in impurities [32]. The bacteria secrete cellulose nanofibers with width of smaller than 100 nm. Thus it provides several advantages compared to the cellulose fibers retrieved from wood or plant matter. Being pure cellulose, the purification and isolation processes are not required. It can be used as-grown, thus retaining all property advantages that native cellulose has over processed cellulose, among them the high degrees of crystallinity and polymerisation. The possibilities to tailor the structure and properties of the fibers during synthesis are discussed in the next section.

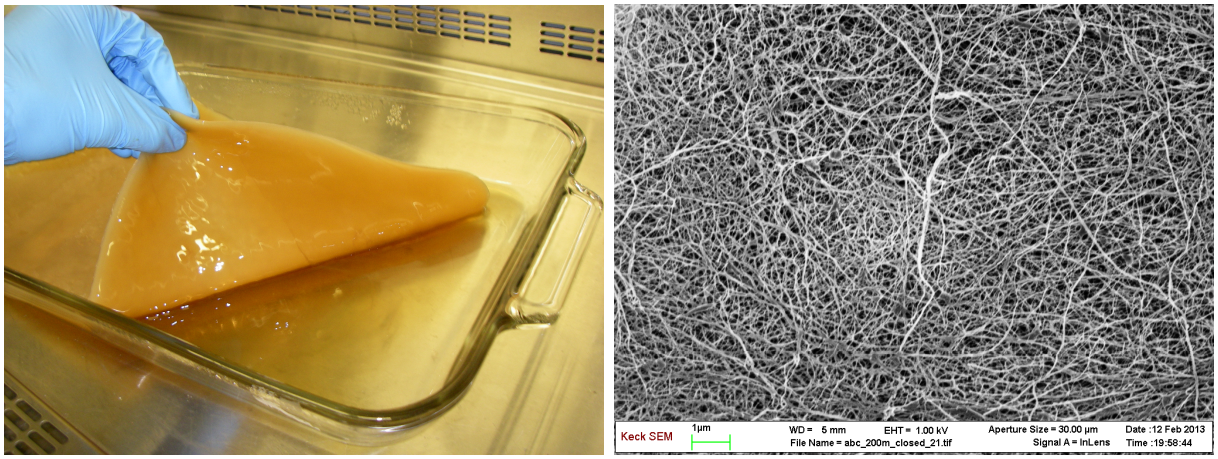

Figure 1.6: A thick cellulose pellicle being removed from the culture medium [35] (left) and an SEM image of fiber mesh that makes up a pellicle.

1.2 Synthesis

Bacterial cellulose is, as the name suggests, produced by bacteria. There are several species of cellulose synthesizing bacteria reported [33], but Acetobacter xylinum is the species that is almost exclusively used for producing BC. This was the first bacterium to be discovered to synthesize cellulose by Brown [5] in 1886. The genus Acetobacter is generally known for the ability to ferment ethanol into acetic acid and are ubiquitous in the production of vinegar [34]. However, some species in the genus have the ability to synthesize cellulose. A. xylinum is the most efficient cellulose producing bacterium known. It is a rod-like, aerobic bacterium with length of up to 4 µm and diameter smaller than 1 µm. The fermentation of sugars in an A. xylinum culture results in a mat like structure called a pellicle shown on the left in figure 1.6. The biological function of this pellicle is said to protect the bacteria from drying out due to the water holding capability and help to keep the bacteria in the oxygen-rich surface region of the medium [2]. This pellicle is also sometimes referred to as a biofilm or membrane. The pellicles can get several cm in thickness depending on the growth time. Laterally it is only confined by the expansion of the growth vessel.

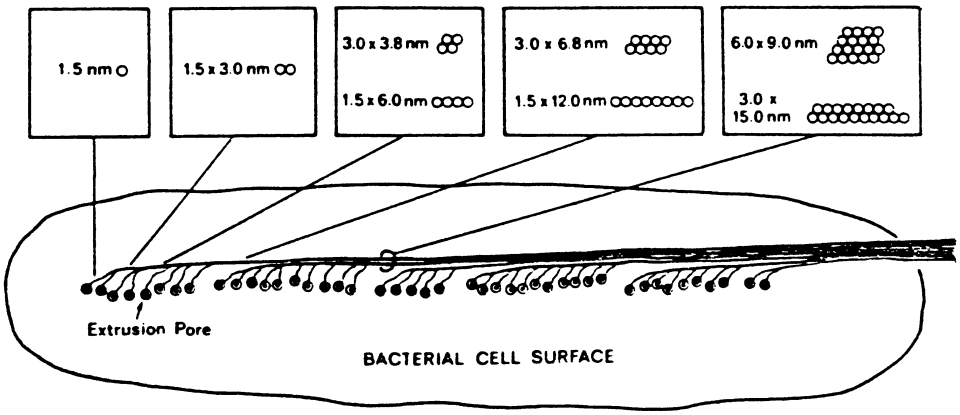

Figure 1.7: Schematic of cellulose nanoribbon forming outside the bacterial cell. Each strand is an elementary fibril that aggregate to form a microfibril and then a nanoribbon [32].

The pellicle is an interwoven mesh of nanofibers as shown on the right of figure 1.6. The cellulose molecules are synthesized inside the cell wall and then extruded and assembled into elementary fibrils first. These fibrils are combined to form microfibrils. Microfibrils are composed of 10 to 250 polymer chains that have been arranged in a parallel array [32]. Those fibrils are then put together to form a nanofiber. The hierarchical assembly is shown in figure 1.7. As investigations have shown the width of the fibers is up to ten times the height [36]. As a result, the nanofibers are also referred to as nanoribbons. Generally the dimensions of these ribbons are 50 nm to 150 nm in width and 5 nm to 10 nm in height.

The yield of cellulose, rate of growth and degree of crystallinity among other properties, depend on a multitude of variables among which are the medium composition, the content and form of the carbon and nitrogen sources, the pH, temperature and time of incubation, the air-liquid surface to medium volume ratio, the specific strain of Acetobacter and culture agitation [37]. The complexity of the process forbids any kind of best configuration but depending on which material property is supposed to be optimized determines what the parameters of the growth process should be. To optimize the process some trials are necessary since all the variables are inter-dependent. For example not every strain will

give the best yields for the same carbon source as various publications have indicated [37]. Even though, the pioneering work of Hestrin and Schramm [38] led to a defacto standard culture medium for the cultivation of A. xylinum. The so called Hestrin-Schramm medium consisting of $2\,\%_{\mathrm{w/v}}$ of glucose and $0.5\,\%_{\mathrm{w/v}}$ of both Bactopeptone and yeast extract at slightly acidic conditions (pH 6) yielded exceptional amounts of cellulose in static cultures. Only since the early 1990 were efforts being made to investigate the variables in cellulose production with the proposal of different medium compositions. Embuscado et al. [39] tried with some success to computationally optimize the cellulose yield for one A. xylinum strain through response surface methodology which tries to predict optimal conditions for a given set of variables via experimentally determined data. While they were able to optimize the cellulose yield for their cultivation environment, the specificity of the results to the strain and the amount of effort prohibited this method to be more widely used.

Even though yield in an agitated culture can be higher than in a static culture [40, 41] and the ability to adjust the conditions during cultivation like aeration and medium concentrations [42, 43] are beneficial for BC growth, the properties of the resulting cellulose do suffer. A comprehensive investigation of a wide variety of strains of A. xylinum to find the one that produces the most cellulose under agitated conditions was conducted by Toyosaki et al. [44]. They tested several thousand strains. The most productive strain, named BPR-2001, is now mostly used for agitated culture experiments. However, crystallite and microfibril size decrease in an agitated culture and the cellulose $\mathrm{I}_\alpha/\mathrm{I}_\beta$ ratio is shifted towards the more stable cellulose I_β [45]. Furthermore agitation of the culture medium leads to lower Young's moduli of the pellicles [18], if a pellicle can be produced at all [45]. These detrimental effects as well as the costs involved in keeping the culture continuously agitated are the reasons that BC production in research environments is overwhelmingly done in static cultures. Though, commercial viability of BC mass production is most likely

only achieved with complex bioreactors [46, 47]. This is why there's an ongoing effort to optimize BC cultivation in agitated conditions. Further discussions in this subsection about BC production and its variables refer only to static cultures.

The carbon source plays a major role in the biosynthesis of BC and is thus a crucial factor affecting the yield. Even though there have been several investigations, the results are not definite. Embuscado et al. [48] found that in their investigation fructose and sucrose produced the largest amount of cellulose and that glucose yielded less than a fifth. However, in another study Masaoka et al. [49] concluded that glucose was the best source closely followed by fructose and glycerol. Sucrose only produced a third of the amount of glucose in their study. Oikawa et al. [50, 51], on the other hand, found that arabitol and mannitol yielded more than six and three times as much as glucose, respectively. A general concern with refined sugar sources is the associated cost. Exploration of other low-cost sources which take advantage of the fact that cellulose production is not tied to a specific source have resulted in a number of alternatives. Hong and Qiu [52] used konjac powder as their precursor and found depending on the pretreatment of the powder that it yields up to three times the amount of glucose as a source. Qiu and Netravali [53] investigated soy flour extract (SFE) which is a waste product of soy bean processing. It contains a variety of sugars among them glucose, fructose and sucrose. They found that A. xylinum prefers glucose and fructose and only utilizing higher order sugars at low concentrations of the former two. The BC yield in a SFE medium was found to be comparable or better than that obtained with pure sugars. The differences in cellulose yield in each study clearly indicate that this is not a simple relationship but highly dependent on various other factors as mentioned above. An advantage of the multiple usable carbon sources is the possibility to easily use waste products from the agriculture industry to produce cellulose [54, 55]. This would improve commercial viability of BC since these by-products of agricultural and

food industry can be inexpensive compared to refined sugars.

Temperature and pH of the culture medium also have an effect on BC productivity. Being an acetic acid bacteria, it was earlier concluded that an acidic pH was beneficial to the survival of the Acetobacter. That, however, is not necessarily indicative of the optimum pH for cellulose production. The investigations performed [49, 48, 37] concluded that a pH of 4 to 6 is preferable for BC production. Most often a pH of 5 is chosen. Cellulose production is generally reported to stop after around 14 days. The rate of production is highest during the first seven days and then tapers off, often stopping after around two weeks [56].

Some other investigations of various other variables showed lesser effects. An analysis of the effect of the nitrogen source on yield revealed that peptone, tryptone and yeast extract were the most favorable sources resulting in increased production compared to inorganic sources [48]. Corn steep liquor (CSL) has also been proposed as a low cost alternative to conventional nitrogen sources [44]. While static cultures didn't show any difference between a CSL-fructose and a conventional medium, CSL-fructose improved yield in agitated cultures. Watanabe and Yamanaka [57] found that a 10 % to 15 % lower oxygen content in the cultivation environment compared to regular atmosphere were beneficial for cellulose production. The surface to volume ratio of the incubation medium can also affect the overall yield but there is no clear relationship known and reports have varied greatly on this [58, 56].

Investigations on the crystallinity of the cellulose fibers depending on the medium composition were performed by several researchers. Ruka et al. [56] reported significant differences in degree of crystallinity ranging from 50 % to 95 % in different media. Cellulose I_α/I_β ratio also differed but the change was not consistent with degree of crystallinity. On the other hand, Mikkelsen et al. [59] didn't see big changes in crystallinity and polymorph ratio with different carbon sources. Molasses and corn steep liquor were proposed to yield

cellulose with higher crystallinity than conventional sources [60].

At the end of the incubation period the bacteria have to be deactivated to prevent further growth of cellulose at unfavorable conditions. In effect, this is a sterilization step to ensure biocompatibility. This is commonly done by boiling the pellicle in 1 % (w/v) solution of NaOH. While NaOH degrades cellulose at high concentrations, at $1\,\%_{w/v}$ it has little effect on the mechanical properties [61].

Bacterial cellulose for the experiments performed in the present research was produced in a medium of 2.5 % D-Mannitol, 0.5 % tryptone and 0.5 % yeast extract in deionized water. This is basically the original Hestrin-Schramm medium with a different carbon source and tryptone instead of peptone [38]. The pH of the solution was lowered to 4.9 pH to 5.0 pH using 10 % acetic acid. The medium was sterilized in an autoclave for 20 min at 15 psi and 121 °C. Bacteria inoculation was done in a sterile bio safety cabinet. A. xylinum from a seed liquid was used to inoculate the medium. The incubation temperature was set to 29.5 °C and left to grow for 1 to 7 days. The bacterial cellulose was grown in conical beakers forming round pellicles and in tubes in tape form.

1.2.1 Directed growth

The mechanism of movement for A. xylinum bacteria is propulsion via the extrusion of cellulose fibers [62]. The movement speed was determined to be around $2\,\mu m\,min^{-1}$ to $4\,\mu m\,min^{-1}$ [36, 63]. This propulsion results in random movement depending on the place of extrusion on the cell wall and the environmental obstacles. Thus the natural form of bacterial cellulose is an interwoven mesh or network with randomly oriented fibers as seen in figure 1.7. Thus, the pellicles nominally have isotropic properties in the plane of expansion. If this is not desirable it is possible to some degree to force the bacteria to move in a more directional manner by a variety of methods.

Kondo et al. [64] used a "nematically ordered" cellulose template to make the bacterium move unidirectionally caused by the interaction of the extruded cellulose microfibrils with the template. Their approach resulted in the bacterium moving in a straight line for about 100 µm before leaving the template direction. The template consisted of parallely ordered glucan chains which the extruded cellulose microfibrils adhere to and thus forces the bacterium to move along the molecular chain direction. An effect of this template is that the microfibrils never assemble into a cellulose nanofiber but stay somewhat separated on top of the template.

Another approach has been to electromagnetically control the movement of the bacteria. Sano et al. [65] found that A. xylinum can be directed by applying an electrical field during cellulose production. The bacteria preferentially move along the electric field thus creating a relatively unidirectional pellicle. Further evidence of this phenomenon was shown by providing a fixed starting point for the bacteria. A BC overgrown string was placed in between two electrodes and the resulting growth of the pellicle was preferably towards the anode [66].

Putra et al. [67, 68, 69] did a series of experiments of growing BC at the interface to another oxygen-permeable liquid or even a solid. They used highly viscous silicone oil, a silicone tube and a ridged PDMS structure. Under certain conditions this resulted in an increase in directionality of the BC fibrils. While it is not clear why BC grown at the interface with silicone oil or the curved silcone surface shows improved orientation, the ridges in the PDMS surface provide a constraint for the bacteria which forces them to move along the ridge direction.

Expanding on these results a series of own experiments were launched to further investigate the possibility of directing the bacteria along a given path. A series of small culture chambers were built as seen in figure 1.8. The chambers were filled with inoculated culture medium

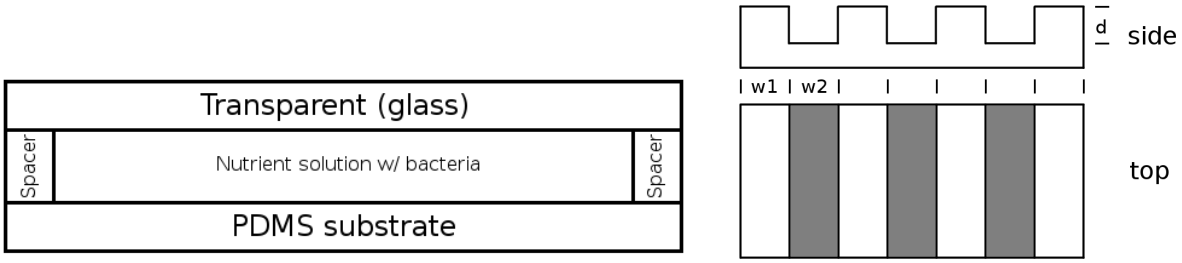

Figure 1.8: Schematics of the culture chamber with PDMS seal (left) and the patterned PDMS substrate (right).

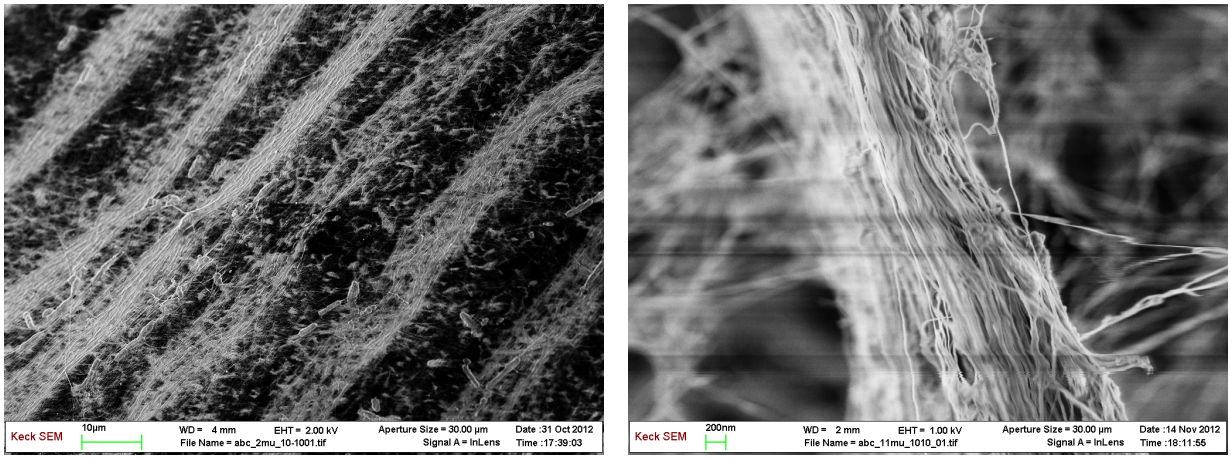

Figure 1.9: Directional strands of bacterial cellulose with at trench depth of 6 µm (left) and 11 µm (right). The width was 10 µm for both.

and then sealed with a thin layer of PDMS that would allow diffusion of oxygen. The PDMS layer was patterned using lithography with ridges or channels of variable width, depth and pitch (see figure 1.8) and functioned as the only oxygen supply route for the bacteria.

While the pitch didn't seem to affect the movement of the bacteria, width and depth could be set to produce highly directional lines of bacterial cellulose. For width and depth of greater than 5 µm the bacteria that found themselves in the trenches were forced to stay there and move along the provided channel. The resulting directional strands of BC can be seen in figure 1.9.

Sakairi et al. developed a direct harvesting method for bacterial cellulose to spin filaments at a continuous rate from the cultural medium [70, 71]. They were able to spin continuous filaments with diameters of about 50 µm to 100 µm with Young's moduli of up to 14 GPa at a wind-up rate of about 16 mm h^{-1}. This is considerably faster than reported production rates of single bacteria, which are reported to be around 2 µm min^{-1} [72, 36]. There was no investigation about this discrepancy.

1.2.2 Drying

The as-produced pellicles are highly porous and due to the hydrophilicity and large surface area of the BC nanofibers have a very high water holding capacity. They are hydrogels incorporating about 99 % water into their structure [73]. For some applications, the pellicles have to be dried, however. Drying of BC pellicles can be done in a few different ways. Most commonly done are evaporation drying at elevated temperatures or freeze-drying.

While oven-drying is less complex it results in a change of morphology of the pellicle. During evaporation of water the porosity of the pellicle is steadily reduced. The surface tension of the evaporating water forces the nanofibers to come closer thus greatly reducing pore size. The porosity is reduced from over 90 % to below 70 % [74] during evaporation drying.

Freeze-drying mostly prevents the reduction in porosity resulting in what is sometimes called an aerogel [75]. In this process, the never-dried pellicle is frozen and then put in a vacuum at very low temperature. Under these conditions sublimation of the water is achieved avoiding the liquid gas transition. This retains the morphology of the pellicle due to the reduction of surface tension and hence the movement of the nanofibers. For even better results a solvent exchange is often done. The pellicle is first immersed in ethanol and then in tertiary butyl (t-butyl) alcohol [76, 77]. T-butyl alcohol has a much

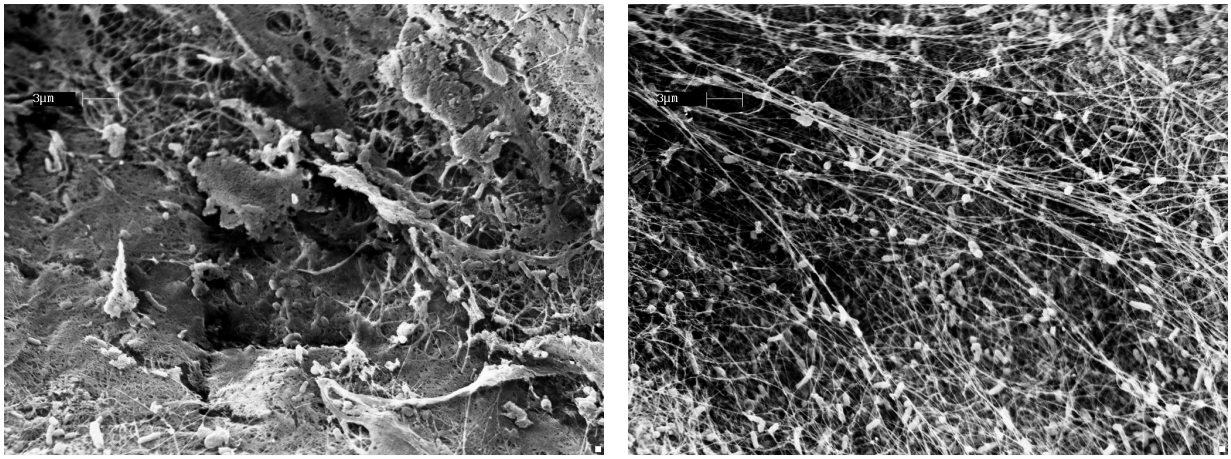

Figure 1.10: Morphology of freeze-dried BC in H_2O (left) and in t-butyl alcohol after solvent exchange (right).

higher vapor pressure and lower surface tension than water rendering it better suited to freeze-drying. Porosities of freeze-dried aerogels can be as high as 98 % [75]. Figure 1.10 shows comparative images showing the morphologies of freeze-dried BC in water on the left and in t-butyl alcohol after solvent exchange.

Supercritical carbon dioxide drying is another alternative method that results in similar structures as freeze-drying. After a solvent exchange of water to ethanol to liquid CO_2, the CO_2 is evaporated beyond the critical point. The resultant aerogels have very low densities due to their high porosity and only exhibit very little shrinkage during drying [78].

1.3 Properties

The mechanical properties of cellulose are dependent on a variety of factors, the source and treatment during production being the main. Every cellulose structure is a mixture of amorphous and crystalline regions as explained above. This ratio along with the specific polymorph of the cellulose play a crucial role in the final properties of the product, i.e. the fiber. Furthermore the DP and impurities present exert an influence on the properties as

well [19, 79, 80]. Environmental conditions also affect the properties of the fiber. Cellulose, with six hydroxyl (OH) groups per cellobiose unit, is sensitive to humidity as the amorphous regions readily absorb water that alters the modulus and strength. In an extensive study of the crystalline regions, Takashi Nishino et al. [81] found that the elastic modulus of cellulose I crystals to be 138 GPa. Crystals of cellulose II, on the other hand, showed a significantly lower modulus in the same study. The authors calculated it to be 88 GPa. Bacterial cellulose is pure cellulose I with high crystallinity and high degree of polymerization. For single bacterial cellulose nanoribbons a Young's modulus of 78 ± 17 GPa was calculated with three-point bending tests using an AFM in force mode [82]. A doubly-clamped fiber suspended over a trench was depressed with an AFM cantilever with known spring constant at different positions along the fiber. The crystallinity of the fibers was estimated to be 60 % using X-ray diffraction. Raman spectroscopy techniques were also used to determine the Young's modulus of single filaments [83]. The estimate of 114 GPa was obtained by relating the shift of the 1095 cm^{-1} Raman band associated with the glycosidic linkage in cellulosic materials to different strain states of the fibers. Fiber crystallinity wasn't investigated. In comparison, the 1095 cm^{-1} band shift was used to investigate the Young's modulus of microcrystalline cellulose (MCC), which consists of polymorph II [84]. The result was an estimated modulus of 25 ± 4 GPa. The crystallinity of the cellulose was reported to be about 48 %. These are promising results for a high modulus, high strength polymeric material based on cellulose I. However, unlike the methods used above which estimate the modulus of single fibers, the pellicles obtained when growing BC in a flask exhibit a random network of nanoribbons that are generated by the random movement of the bacteria. The pellicles have also been investigated as a whole. For example, Yamanaka et al. [85] found that after air-drying or hot-pressing the pellicles the Young's modulus of these was consistently over 15 GPa and when treated with NaOH it increased to 25 GPa [86].

Combining NaOH and NaClO yielded a further increase to nearly 30 GPa. In as-produced, wet form, the BC pellicles have a drastically lower modulus in the range of 1 MPa to 3 MPa [87, 88, 89]. This is mainly due to extensive swelling in the wet state [87, 90] which results in a reduced number of load bearing fibers per unit area. Furthermore, slippage of fibers is greatly enhanced leading to a higher strain at fracture as well as lower strength and modulus. The fibers themselves are experiencing only little change in strength and strain in either condition [91].

Since cellulose is often used in medical applications, which will be discussed in more detail in subsection 1.4, the in vivo biocompatibility is a crucial factor. In 1989 Miyamoto et al. [92] investigated the foreign body reaction and adsorption of cellulose inside a living body for regenerated cellulose and its derivatives. While the biodegradability was dependent on the crystallinity and morphology with highly crystalline cellulose basically not being adsorbed at all after the test period, the foreign body reaction was consistently low no matter what variant was used. Studies of bacterial cellulose biocompatibility mirrored the initial findings. No inflammatory reaction was seen at BC implantation sides and the high crystallinity hindered any kind of degradation in vivo [93]. This was expected because of the high purity of the BC. Further, due to the porous structure of the BC sheets, cells migrated into the structure essentially incorporating the BC filaments into the body seemingly without any negative effects.

1.4 BC applications

While cellulosic material is widely used in paper and textile products, BC is still a niche material which is rarely used in commercial products. This is mainly because of the associated production costs which is due to immature mass production technologies and a general unfamiliarity with it considering its relatively obscure nature compared to other

products. As mentioned above BC finds its biggest use in food products, most notably nata de coco where A. xylinum is the cause of the fermentation of coconut water [11]. Apart from nata de coco, A. xylinum is an essential ingredient in Kombucha where it again helps with fermenting of the tea medium [94]. Additionally BC can be added to food products as a low-fat dietary supplement and to improve the texture [95]. Similarly it is added to cosmetics as a stabilizer [37]. Aside from these low-tech uses, BC is also commercially used in medical, acoustical and composite applications.

In 1988, Sony patented the use of bacterial cellulose as a molding material [96] which was subsequently used in several high-end headphones [97, 98]. Diaphragms made out of BC were used due to their high dynamic strength combined with excellent flexibility which results in high fidelity sound. These properties allowed for sonic velocities of metal diaphragms but with the dynamic range of regular paper diaphragms. New headphones with a bacterial cellulose based diaphragm have been produced as recently as 2011. Initial costs for headphones utilizing BC diaphragms were as high as $3000 in early 1990. Recent models by Vsonic Electronic Company are available for below $200 incorporating more than 100 cellulose layers fused together by in one of there high end products [99].

Its biggest area of commercial deployment, however, is in the medical industry as a wound dressing material and as artificial blood vessels. Klemm et al. investigated the possibility of tubes of bacterial cellulose as artificial blood vessels [4]. Materials that are used during operation as prosthesis have to fulfill numerous requirements. As mentioned above, biocompatibility is crucial and studies of long-term biocompatibility have shown no adverse effects in mice [100]. Further, when used as blood vessels, blood compatibility and impermeability as well as withstanding the blood pressure are required. In a series of tests on rats, as-grown and never-dried bacterial cellulose tubes were used in microsurgery to close arteries and protect repaired nerve strands [4]. The authors showed that in both cases

the BC tubes were incorporated into the organic structure. Regular blood vessel tissue covered the inner wall of the tube without causing any inflammation or immune reaction. The results were identical when protecting a nerve strand. Additionally, it was successfully tested that the BC tube was able to function as a drug delivery system enhancing the recovery rate.

BC films for skin wound healing have been commercially available for more than two decades [101]. They show advantages over other commercial products due to immediate pain relief, transparency for wound inspection bacterial barrier and good adhesion to the wound bed among others [102].

Further investigations have targeted BC films as a scaffold for tissue engineering and growth. As a scaffold for skin engineering, BC has all the advantageous it has as a wound dressing application and additionally is easy to produce very cost-efficiently and doesn't require any involved processes to be applicable [103]. As the porous structure of a BC film can be penetrated by human tissue, it can be permanently implanted without toxicity or inflammatory issues for the human body [88]. Promising results were obtained when investigating the potential for cartilage growth [104] and for BC-hydroxyapatite composites to guide bone regeneration [105]. An advantage of BC in scaffold applications is its malleability. Temporary paraffin wax microspheres were used to increase pore size of BC pellicles which improves cell penetration and mineral deposition inside the scaffold [106].

BC nanofibers have been investigated as a reinforcement material in green composites [55]. It meets all the requirements to be used as a reinforcement in composites and especially for green composites where matrix and reinforcement are entirely made from sustainable and biodegradable materials. Conventional composites often consist of an epoxy matrix and fiber reinforcements such as Kevlar®, glass fibers or carbon fibers. These materials are all extremely competent reinforcements but with increasing use of composites in technological

applications, the problem of waste cannot be ignored as these materials basically do not degrade under natural conditions Dumped in landfills at the end of their life, the synthetic fibers and resins in conventional composites can stay as is without degrading for several decades, if not centuries.

Investigations of cellulosic materials with high aspect ratio in composites began nearly two decades ago with first successes reported by Favier et al. in 1995 with tunicate cellulose in the form of rods with lengths in the micrometer range and widths of about 10 nm to 20 nm [107]. From there all kinds of cellulosic precursors were investigated. Bacterial cellulose was part of that investigation in various ways.

BC was used to create hierarchical reinforcement materials. BC was grown in the presence of sisal and hemp fibers [108]. After cultivation the fibers were "coated" with BC. This actually decreased the fiber properties but increased the interfacial shear strength of matrix and reinforcement thus resulting in a higher pull-out force. This was shown to improve mechanical properties of composites with PLLA [109].

Bacterial cellulose has also been used as a standalone reinforcement material [55]. Nakagaito et al. have found that bacterial cellulose has an advantage over other forms of cellulose when used in composite materials [110]. This is due to the unique structure of BC which features high aspect ratio fibers in a non-woven structure. They found that BC reinforced composites have generally higher tensile strength and modulus than equivalent composites with microfibrillated cellulose. Another advantage of the nanofiber structure of cellulose is the optical transparency. Yano et al. combined impregnated bacterial cellulose sheets with epoxy resin and were able to produce highly flexible transparent composite films. The reduction in transmission in the BC impregnated film compared to only epoxy was less than 10 % [111]. Additionally, they claimed that these films were five times as strong as other engineering plastics in terms of Young's modulus. Other transparent composite films were

engineered using chitosan as the matrix [112]. Chitosan is a derivative of chitin and thus very similar in structure to cellulose as well as renewable, biodegradable and biocompatible. The composite was made using green processes. The results were similar to composites with epoxy where the incorporation of BC resulted in an increase in the mechanical properties while maintaining most of the transmittance dropping from 90 % to 70 % at 30 % fiber loading. Other investigations into BC reinforced biodegradable composites focusing on mechanical properties showed similar increases and additionally the ability to control the properties based on the cross-linking of the matrix and reinforcements [3]. Fully sustainable composites using thermoplastic starch as the matrix are also under investigation [113, 114]. Again bacterial cellulose delivers the best results in comparison to other cellulose forms in terms of strength and modulus. A problem that arises with these fully green composites, however, is their high water absorption. Since both matrix and cellulose are hydrophilic, high humidity results in swelling of the composites and associated decrease of mechanical properties. While most researchers utilized solution based processes to impregnate the cellulose sheets with starch, Grande et al. incorporated the starch during the A. xylinum cultivation and thus bacterial cellulose growth [115]. BC is still produced in the presence of gelatinized starches while preserving morphology and properties of the cellulose fibers. Another step further is the design of an all-cellulosic composite where cellulose is both the matrix and the reinforcements. After first reports with plant-based cellulose [116]. Soykeabkaew et al. used BC to create such a composite [117]. They used a surface selective dissolution method where a suitable solvent dissolved the surface of the cellulose fibers to form the matrix material. The immersion time determines how much of the fiber surface layer is dissolved. They were able to produce composites that improved the properties of the original BC sheets in strength, strain and toughness. These composites compared favorably to other all-cellulose composites from different sources.

Other emerging applications include BC based carbon fibers which is discussed in detail in chapter 2 as well as harvesting energy using a BC cantilever. This is examined in chapter 3.

2 Cellulose based carbon fibers

In 1879, Thomas Edison while working on the first incandescent light bulb was the first man to purposefully use a carbon fiber [118]. As a filament for the light bulb he baked cotton or bamboo threads, which carbonized the cellulose in the threads. While an electrical current was applied the carbonized threads would heat up and glow. In the 1950s then, the first commercial carbon fibers were manufactured from cellulose, specifically rayon which is a type of regenerated cellulose. However, these suffered from poor properties. First evidence of high strength fibers was published in 1960 when Bacon [119] grew graphite whiskers of several centimeter in length in an arc discharge process. He reported tensile strengths of up to 20 GPa and Young's moduli reaching 700 GPa. This sparked renewed interest in carbon fibers mainly focused on viscose rayon as a precursor and eventually led to the entry into the composite market in the early 1960s [118]. At the same time, the first successful demonstrations of carbon fibers from polyacrylonitrile (PAN) precursor were reported [120, 121]. This led to the replacement of most rayon based fibers due to better properties and lower manufacturing costs for PAN based fibers which dominate the market to this day [118]. Rayon based fibers on the other hand make up only a tiny amount of carbon fibers produced today [122]. In the late 1970s, so called mesophase pitch, a kind of liquid crystalline phase of carbonaceous pitch, was discovered to be suitable for spinning fibers and being graphitized to yield high modulus fibers [123, 124]. Mesophase pitch and

PAN are the two precursors that are most widely used, especially in high performance applications like composites. Rayon is mainly used for activated carbon applications where strengths isn't a crucial factor. Other precursors have been investigated but nothing has provided the same properties-cost package that PAN delivers [125].

Carbon fibers are the most widely used fiber reinforcements in advanced composites. Carbon fiber reinforced polymers/plastics (CFRP) are deployed especially in high performance applications like the aerospace sector with new models from Airbus and Boeing now employing more than 50 % of composites in weight, mostly CFRP, in their structure [126, 127, 128]. But demand also comes from more general applications like automobiles, sports gear and in civil engineering [125]. With ever increasing utilization of CFRPs, the carbon fiber market is expected to continue to grow in the coming years [129, 99]. However, a challenge for the industry is still the high cost of production, the dependence on fossil fuels for the precursors and the waste accumulation as commercial CFRPs are non-biodegradable. Part of the problem of biodegradability is the epoxy matrix used in most composites. There is an ongoing effort to come up with new and environmentally friendly matrix materials as discussed in the last chapter. The carbon fibers themselves are also non-biodegradable which is an inherent problem for high performance composites. Since biodegradable fibers don't have the required properties to replace carbon fibers, green precursors would be a means to reduce the dependence on fossil fuels and the cost of production and provide a carbon dioxide neutral way to carbon fiber manufacturing. There have been few efforts based on lignin, cellulosic and recycled materials [130, 131]. While these have shown potential and some progress has already been made, they cannot yet compete with commercially available PAN based fibers. Apart from the properties the cost factor for these new precursors is important since both PAN and pitch are expensive making up more than half the cost of manufacturing [132]. There's potential for a low cost renewable precursor to disrupt the

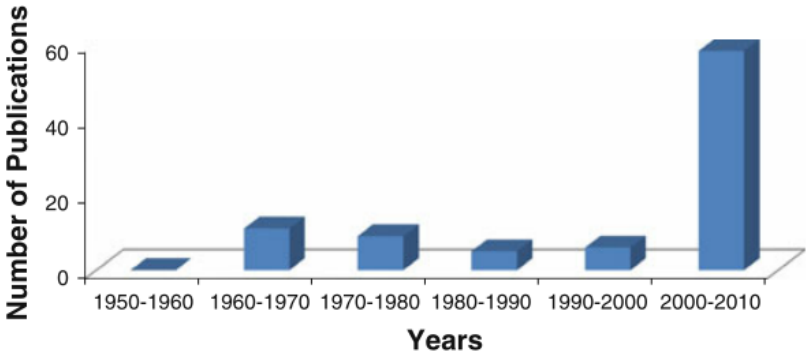

Figure 2.1: Number of research publications on carbonization of cellulosic precursors [132].

status quo.

Rayon based fibers are only utilized in niche applications these days. However, cellulose research hasn't stopped in the last half century. Since it is ubiquitous, costs for cellulose precursors can be reduced. Further, due to its variety in structure and morphology as well as its malleability there may be potential to optimize it to offer a good balance between cost and properties to become commercially viable. This is reflected in a rapid increase in publications about carbonization of cellulosic precursors in the last decade as seen in figure 2.1.

2.1 Precursor-structure relationship

The structure of the precursor is fundamental in determining the resulting structure and properties of the carbon fiber. Carbon fibers are basically 100 % carbon in the form of graphene sheets, which are one atomic layers of carbon in a hexagonal crystal structure [133]. Depending on whether the precursor is graphitizing or non-graphitizing the carbon fiber can have either graphitic, turbostratic or a hybrid structure [134, 135].

In graphite the sheets are planar in a three dimensionally stacked order. The d-spacing is 0.335 nm, the in-plane Young's modulus for a perfect single crystal has been calculated

to be around 1060 GPa. If a material produces a carbon fiber with a similar structure it is called a graphitizing precursor. One example would be mesophase pitch. The graphitizing nature of pitch is the reason for the high moduli achievable from this precursor [136]. The polycrystallinity of the fibers leads to a lowered modulus but can still surpass 900 GPa [137].

Non-graphitizing precursors result in a turbostratic structure in which, unlike graphite, the graphene layers are not necessarily planar. They can be bent, folded or crumpled and exhibit rotational disorder from one layer to the next resulting in only two dimensional order as shown in figure 2.3. This results in a lower modulus but comparably higher strength. PAN is the prime example for this behavior [138]. High strength PAN fibers reach more than 6 GPa tensile strength [139].

Cellulose has been considered as a non-graphitizing precursor [140]. However, most of the studies on cellulosic precursors have focused on low crystallinity regenerated cellulose. The few reports on graphitization of highly crystalline cellulose like tunicate or bacterial cellulose have not investigated the resulting structure of the carbon fibers in depth [77]. Investing PAN and mesophase pitch derived carbon fibers is useful to gain further inside into the precursor-structure relationship.

2.1.1 PAN derived carbon fibers

PAN is a linear polymer with a pure carbon backbone and nitrile groups periodically branching off. The chemical structure of PAN is shown in figure 2.2. Its nitrile groups are highly polar [142]. Therefore it has a high glass transition and melting temperature. In fact it usually decomposes before melting. Commercially a copolymer of PAN and other additives such as methyl acrylate and vinyl acetate are used in manufacturing. This is to tailor the properties of the resulting carbon fiber by altering the ordering in the initial fiber.

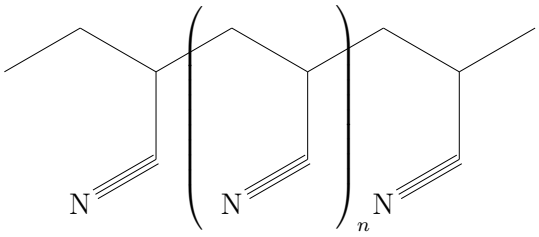

Figure 2.2: Polyacrylonitrile (PAN) chemical structure

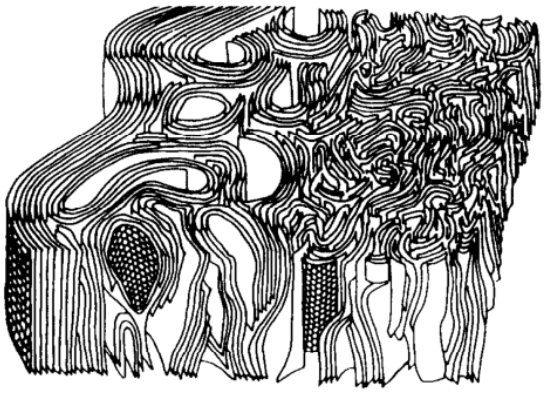

Figure 2.3: Layered stacking in PAN as proposed by Johnson [141].

Additionally they affect other properties including melting point, solubility and oxygen permeation [142]. Since the amount of the copolymer is rather small, the carbon fibers are generally referred to as PAN-based. PAN is spun into a fiber through one of three spinning processes: melt, dry and wet spinning, melt spinning being the preferred method since it doesn't involve solvents [143].

Carbon fiber production can be divided into three stages, which are similar for all precursors: stabilization, carbonization and graphitization [144]. The stages differ to a varying degree between precursors with stabilization differing the most and graphitization being very similar. In the case of PAN, during stabilization, the fiber is heated to 200 °C to 300 °C in air. At these temperatures the fiber undergoes three closely linked reactions [143]. Since stabilization is done in air the PAN molecules are at least partially oxidized. Dehydrogenation follows the oxidation process, removing hydrogen atoms in the form of water from the carbon back bone. The resulting double bonds improve stability of the polymer. Following that cyclization is the final step towards obtaining the so called ladder structure. As seen in figure 2.4, the steps can also happen in reverse with cyclization before oxidation and dehydrogenation. The ladder structure is a stable polymer suitable

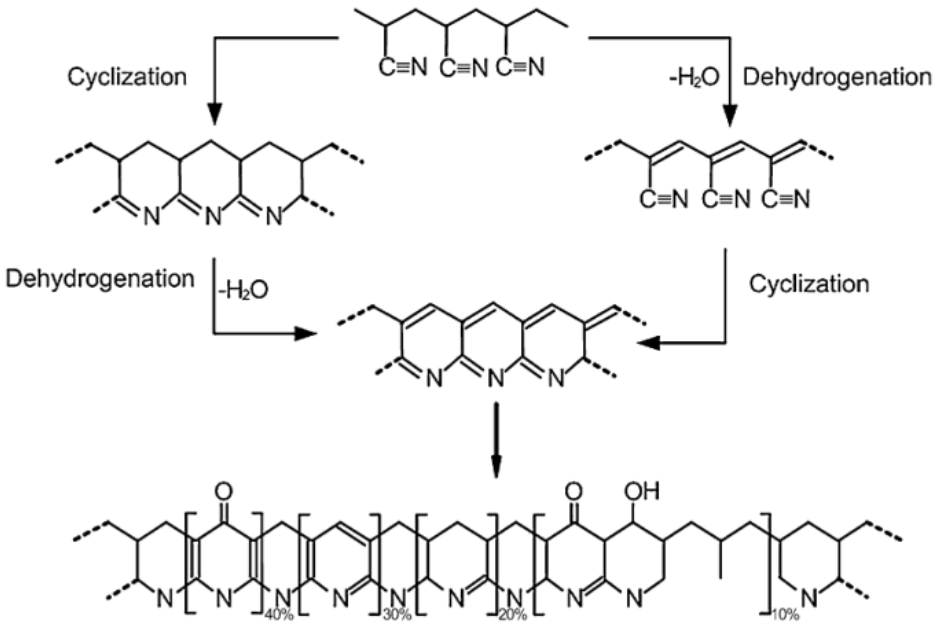

Figure 2.4: Intermediate structures in the two step process of stabilizing PAN at low temperatures (oxidation not shown) [145].

for crosslinking.

The second stage is carbonization. Increasing the temperature in an inert atmosphere, usually N_2, up to 1500 °C removes the majority of non-carbon atoms and leads to crosslinking of the hexagonal polymers into the two dimensional layer structure typical for graphene [144]. If the fiber is being stretched during the process the preferential orientation of the sheets is more aligned with the fiber axis which yields a higher modulus and strength.

Graphitization at temperatures exceeding 2000 °C improves the size of the graphite sheets and further removes impurities and defects in the structure resulting in high modulus fibers. At this stage the mass decreases to 55 % to 60 % of its original value, more than 99 % of it being carbon. The rest of the atoms have been released in gaseous form [143]. Depending on the heat treatment and the initial PAN structure three different fiber morphologies have been proposed. While the preferred orientation of the layers is always along the fiber axis

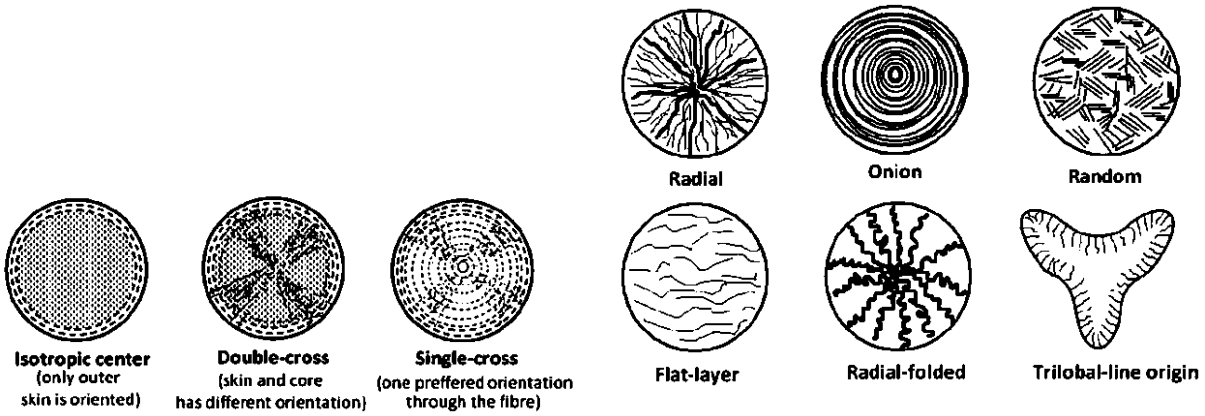

Transverse texture of PAN-based carbon fibers [148].

Mesophase pitch-based fiber transversal textures [143].

Figure 2.5: The transverse textures for PAN and mesophase pitch based carbon fibers. Three distinct textures were found for PAN and six for pitch.

there are differences in the radial texture. PAN-based carbon fibers generally develop a skin-core structure [146]. Three different textures have been proposed [143]. In the skin region, the crystallites are well aligned, but considerable differences are apparent in the core texture. An overview of the different textures is shown in figure 2.5. The resulting structure depends on the precursor structure and process parameters. Generally there's a negative modulus gradient from the skin to the core due to larger and better aligned crystallites in the skin region [147].

PAN based fibers have a tensile strength of up to 6 GPa and moduli of 600 GPa for high strength (HTS) and high modulus fibers (HM), respectively [132]. The major difference in the structure of these two types of carbon fibers is the crystallite size L_a. HTS fibers have crystallite sizes of 10 nm to 20 nm and HM fibers up to 70 nm [149].

2.2 Mesophase pitch based carbon fibers

Pitch is a high viscosity liquid made up of about two thirds aromatic planar oligomers [150]. Originally derived from petroleum or coal, it is nowadays synthesized from suitable monomers like naphthalene and its derivatives to optimize its properties [133]. Pitch is an isotropic material under normal conditions [151]. Upon heat treatment polymerization and condensation reactions lead to an increase in the molecular weight of the oligomers and phase separation occurs in the form of spheres. These spheres exhibit a so called mesophase which is highly anisotropic. The planar oligomers arrange into a stacked order. This mesophase behaves similar to a liquid crystal phase. Depending on the heat treatment all or only a fraction of the pitch is transformed into the mesophase. Unlike PAN based fibers there's not one monomer that is most suitable for producing carbon fibers. Rather it is a mixture of different oligomers with average molecular weight between 300 to 400 [152].

Mesophase pitch can be melt-spun into fibers. The spinning aligns the mesophase domains along the fiber direction. One problem during spinning is the high viscosity of the mesophase compared to the isotropic fraction versus the improved properties with a large amount of mesophase. Optimization of the various parameters is crucial to obtain the desired properties. Singer reported an optimum mesophase fraction of 55 % to 65 % [124].

Carbon fiber manufacturing from pitch follows a similar pattern as PAN. However, the oxidation and stabilization phase at temperatures around 250 °C to 350 °C in air results in the crosslinking of the various aromatic hydrocarbons as well as introducing oxygen containing groups which form strong hydrogen bonds thus strengthening the three dimensional structure [153]. Carbonization is done at elevated temperatures in an inert atmosphere followed by graphitization at up to 3000 °C. Due to the well-aligned precursor structure, pitch is considered a graphitizing material. Unlike PAN, pitch carbon fibers exhibit a three dimensional graphite-like structure after graphitization. This is the main

reason for the improved modulus over PAN CF [154]. Another advantage of mesophase pitch CF is that 80 % to 85 % carbon yield can be achieved.

The spinning process is the most crucial factor to determine the tensile properties of carbon fibers due to the dependence of the resulting structure on the original one [152]. The layers present in the non-carbonized fibers are retained in the final state. Pitch based fibers have several transverse textures, among them radial, random, onionskin and a mixture of these are shown in figure 2.5. The properties of these fibers are dependent on the transverse structure but there is no clear relationship [133]. However Bright and Singer reported that radial structures are more readily graphitizable than random structures [154]. The strong alignment and large crystallite sizes allow pitch based fibers to have a very high modulus exceeding those of PAN carbon fibers. Young's moduli of pitch based fibers can exceed 800 GPa [152]. However the graphite structure apparently limits the tensile strengths to about 3 GPa, only half of what PAN CF reach [132].

2.3 Cellulose based fibers

Cellulose albeit having only 44.4 % carbon content compared to 67 % for PAN and close to 100 % in case of pitch is still a promising precursor for carbon fibers. Due to its ubiquity it is very cheap and depending on the source very pure cellulose can be obtained. While cost and chemical residues is a problem in PAN based fibers, which limits the application potential in some areas [132]. Even though viscose rayon (VR) based carbon fibers hardly play a role in commercial applications due to inferior mechanical properties they are heavily relied upon in military and space vehicles [155]. Applications like heat shields, where VR CF are preferred, depend on good thermal performance and fiber-matrix adhesion more than mechanical properties. These are areas where VR shines. Rayon carbon fibers have a crenulated fiber shape which improves adhesion with the matrix and feature low thermal conductivity as

well as good durability [156]. Rayon is called the first man-made, semi-synthetic fiber [157]. It's semi-synthetic since it is a direct product of a natural material, cellulose. Rayon is a generic name for regenerated cellulose fibers first produced in the middle of the 19th century. Producing rayon via the viscose process results in viscose rayon. The viscose process is complex requiring multiple steps and chemicals. Wood pulp is treated with sodium hydroxide and carbon disulfide to form cellulose xanthate. Cellulose xanthate is soluble in an appropriate solvent and yields a highly viscous solution that can be spun into fibers using wet spinning process. After the spinning the cellulose is regenerated in a bath containing sulfuric acid and other chemicals. After the spinning the fibers are stretched to improve the alignment of the molecules that result in better mechanical properties.

Cellulose undergoes various stages during pyrolysis. Especially in the low temperature region up to 700 °C a high number of processes occur [158]. Similar to the other mentioned CF, it is possible to roughly divide the process into three distinct stages: stabilization, carbonization and graphitization. Stabilization in the case of cellulose is a complex process. Cellulose as the other precursors does not melt before degradation which is important to keep the fiber structure intact. However unlike PAN cellulose suffers from chain scission. The glycosidic bond has to be broken in order to remove the oxygen connecting the glucopyranose units. Tang and Bacon [158] identified four stages during low temperature pyrolysis namely physical desorption of water, dehydration from the cellulose unit, thermal cleavage of the glycosidic linkage and scission of other C−O bonds and lastly aromatization. This general hypothesis of the thermal degradation of cellulose remains largely intact to this day. Due to the inherent hydrophilicity of cellulose, water is stored to some extent inside the structure [132]. This water is removed during the initial heating up to 150 °C. With increasing temperature dehydration from the glucopyranose units follows. The hydroxyl groups from the ring structure are removed, the remaining carbons forming double bonds.

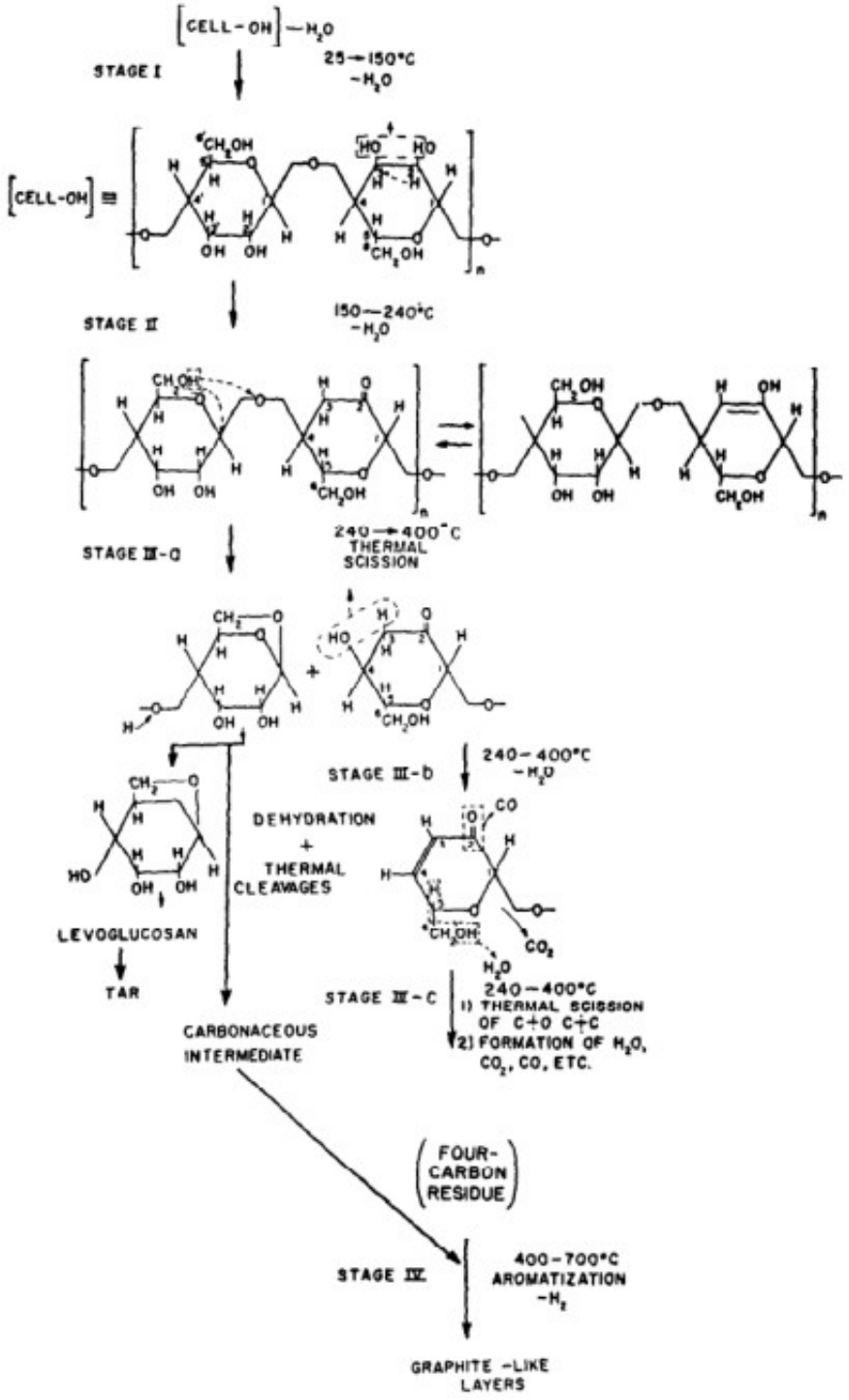

Figure 2.6: Chemical processes during pyrolysis of cellulose as proposed by Tang and Bacon [158].

Thermal scission requires even more energy. The glycosidic linkage is broken up leaving two products. One is similar to levoglucosan which is a precursor for tar. This transformation is undesirable. Further scissions take place breaking C=O and C−O bonds. This is the phase that results in the biggest loss of carbon material due to the formation of volatile compounds. At temperatures above 700 °C repolymerization of the carbon residues begins and aromatization into the hexagonal graphene structure follows. Graphitization leads to the growth of the crystallites and if done under stress leads to good orientation of the stacked layers along the fiber. Graphite layers are formed from the (101) planes of cellulose I [27]. Due to the differing crystal structure of cellulose II there's a 90° rotation necessary in this case. Depending on the molecular orientation along the fiber, the graphite layers are oriented which affects longitudinal shrinkage during pyrolysis.

A crucial step in the manufacturing of high performance carbon fibers from rayon is hot-stretching during carbonization and graphitization [159]. The orientation of the cellulose chains is almost completely lost without an applied load to stretch the fibers and thus improve orientation of the graphite layers along the axis [160]. Thus stress-free graphitized fibers will have vastly inferior properties to stress-annealed ones. The hot-stretching is especially important during carbonization above 900 °C to negate longitudinal shrinkage and yield highly oriented carbon fibers. It is a costly endeavor which was one of the reasons that PAN quickly supplanted rayon as the preferred precursor. Tensile strengths of hot-stretched graphitized rayon fibers achieve up to 2.5 GPa and moduli of more than 500 GPa [152]. This, as seen in the pitch and PAN CF sections, can't compete in terms of modulus or strength, respectively.

Important properties for cellulose fibers to be used as precursors are low defect density like voids and de-bonding, high degree of polymerization, high aspect ratio and preferred orientation of cellulose microfibrils.

Apart from viscose rayon, there are a few other cellulose fibers that have been developed more recently. Of note are liquid crystalline cellulose (LCC) fibers. These fibers are drawn from a solution in which the cellulose forms a liquid crystal phase [161]. Lyocell is a commercial example of a regenerated cellulose fiber that is spun from a solution of cellulose in a tertiary amine N-oxide and water mixture [162] and which has drawn some interest in its suitability as a precursor. This process is environmentally friendlier than the viscose process since the solution can be recovered for reuse. Cellulose can also form a liquid crystalline phase when dissolved in phosphoric acid [163]. The advantage of fibers spun from an anisotropic solution is better orientation and higher crystallinity than comparable viscose rayon fibers resulting in better tenacity and modulus. [164, 165]. Carbon fibers made from Lyocell show promise. For the same process parameters they retain their strength and modulus advantage over rayon [166]. This is attributed to the higher degree of polymerization and a lower defect density of the precursor material. Pyrolyzed LCC fibers show core-skin structure where the skin is graphitic after heat treatment at 2500 °C [167]. The core shows smaller crystallite sizes and reduced properties. This core skin structure remains even at temperatures of 3200 °C [168].

In graphitization experiments done at Cornell University, Alfred University and at Corning Inc. up to 2200 °C in various furnaces under vacuum or in an inert atmosphere, the incomplete graphitization of LCC fibers was confirmed as is shown in the Raman spectra and XRD patterns in figures 2.8 and 2.7.

At 2200 °C the degree to which graphitization can be achieved is limited especially without stress applied to the fibers [169]. Hot stretching has a significant effect on cellulose based fibers increasing degree of orientation, crystallite size and mechanical properties. Without stress-annealing the crystallites are turbostratically ordered and poorly oriented. Hot stretching especially increase L_c giving rise to a more three dimensionally ordered

structure [170].

Viscose rayon and liquid crystalline cellulose are both a form of regenerated cellulose. This type of cellulose suffers from low DP [132].

Native plant based celluloses are also non-graphitizing polymers. They suffer from the same shortcomings as viscose rayon in that the yield is low in untreated condition. The graphite crystallite size supposedly is directly correlated to the original crystallite size of the cellulose. Kim et al. [171] shows evidence of graphitization of BC at 2000 °C.

2.3.1 Characterization of cellulose based carbon fibers

Characterization methods to determine the degree of graphitization usually involve X-ray diffraction (XRD) and Raman spectroscopy, the latter of which also provides an opportunity to non-destructively measure the mechanical properties [172].

XRD gives an estimation of the in-plane size L_a of the graphitic crystallites and out-of-plane dimension L_c, the crystallite height. Furthermore the interlayer spacing d_{002} can be calculated. The pattern is also indicative of the type of microstructure the fiber has, graphitic or turbostratic [173]. To determine the crystallite size, the Scherrer equation is used utilizing the 002 reflection which also corresponds to the interlayer spacing of the crystallites. Crystallite sizes are usually less than 100 nm so Scherrer's equation is applicable. The Scherrer equation is given by [174]

$$L = \frac{K\lambda}{\beta \cos \Theta}, \tag{2.1}$$

where K is a factor that incorporates the shape of the crystallites and is usually around 1.84, λ is the X-ray wavelength, β is full width at half maximum (FWHM) and Θ is the

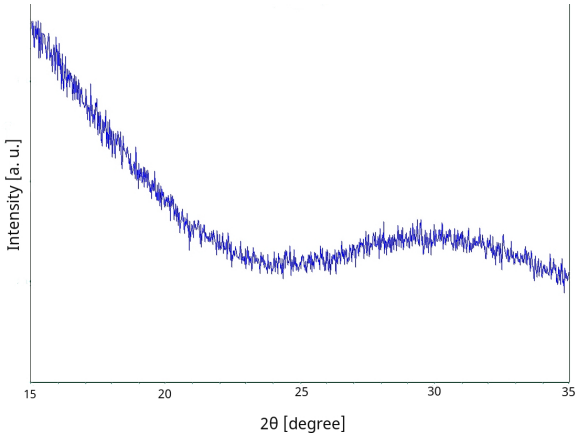

XRD results of a non-graphitized BC-based carbon fiber pyrolysed at 2100 °C in vacuum.

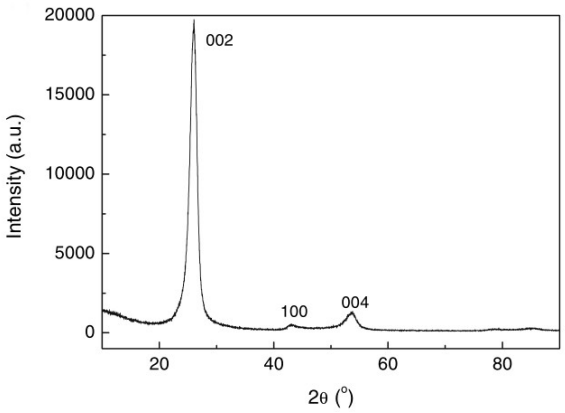

X-ray diffraction scan of commercial grade PAN fibers heat treated to 2800 °C [175].

Figure 2.7: The 002 peak at $2\theta = 26°$ which indicates graphitic structure is missing from the BC-based carbon fiber prepared in the lab compared to commercially available carbon fibers.

Bragg angle. d_{002} is determined via Bragg's law:

$$d = \frac{n\lambda}{2\sin\Theta}. \tag{2.2}$$

For d_{002}, Θ equals around 26°. An appearance of the 112 diffraction peak indicates a three-dimensional ordering which suggest a graphitic crystal structure. If it is missing, a turbostratic structure is present. XRD experiments for this thesis were done in air in a Scintag Theta-Theta X-ray diffractometer utilizing Cu K_a radiation.

Even though evidence of graphitization has been reported for temperatures as low as 2000 °C for bacterial cellulose [171], in experiments up to 2300 °C the strength of the produced carbon fibers was low indicating incomplete graphitization up to these temperatures. This was confirmed via XRD measurements as shown in figure 2.7.

This figure shows the results of an XRD scan from 15° to 35° to check for the existence of the 002 peak of the graphite structure in a heat treated bacterial cellulose fiber. The BC

fiber was pyrolyzed up to 2100°. In comparison, the presence of this peak in a commercial PAN based carbon fiber shows the extent to which intensities the 002 peak is missing in the BC based fiber.

Another technique regularly used for characterizing CF properties is Raman spectroscopy. Tuinstra and Koenig [176] showed that there is an inverse linear relationship between the two primary Raman bands at $1355\,\mathrm{cm}^{-1}$ and $1575\,\mathrm{cm}^{-1}$ and the crystallite size of a graphitic material. These bands are called the D and G bands, respectively. The G band is present in single crystal graphite whereas the D band is missing. The I_D/I_G ratio is inversely proportional to L_a. For the single crystal the crystallite size can be thought of as infinite. Carbon fibers show both bands indicating a finite crystallite size. Even though it is not quite clear if this analysis should be done with the height or the area of the bands [177], a general trend is noticeable with both measures. Raman measurements can be utilized to determine local stress states in carbon fibers due to a linear shift of the G band with increasing uniaxial stress [172]. This allows for the determination of the Young's modulus in a non-destructive manner. Raman experiments were done locally with a Renishaw InVia Confocal Raman microscope using a 488 nm laser.

To double check liquid crystalline cellulose fibers were also pyrolyzed to compare them to BC based fibers. The examination showed identical results to bacterial cellulose fibers. The findings also concur with reports from Kong et al. [167] who found incomplete graphitization in LCC fibers.

As mentioned earlier, yield is one of the major drawbacks to using cellulose as a carbon fiber precursor. The theoretical yield of 44.4 % is hardly achieved due to carbon being removed as volatile carbon compounds. So in inert atmosphere the yield for bacterial cellulose in TGA experiments was below 20 % as shown in figure 2.9.

However there are ways to increase the yield. Bacterial cellulose treated with sulfuric acid

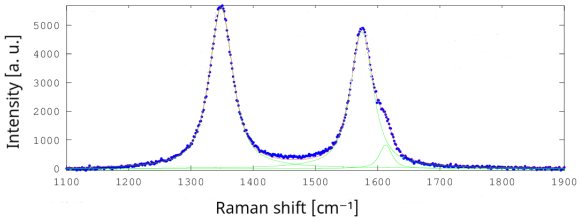

Raman spectrum for BC-based carbon fiber pyrolysed at 2200 °C in vacuum.

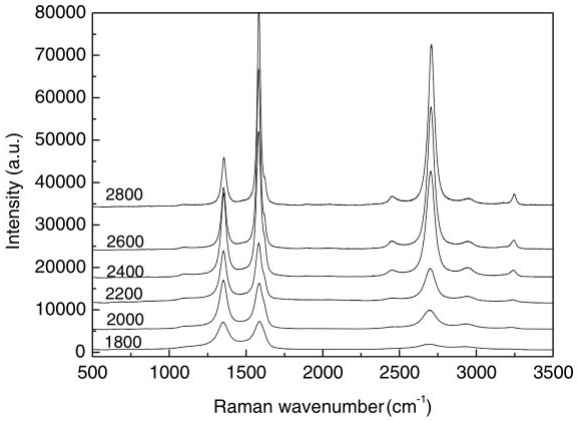

Raman spectra of PAN-based CF pyrolysed at different temperatures [175].

Figure 2.8: The intensities of the Raman shifts at 1580 cm^{-1} (G band) and 1360 cm^{-1} (D band) indicate the degree of graphitization. The higher the G band the farther has the graphitization progressed.

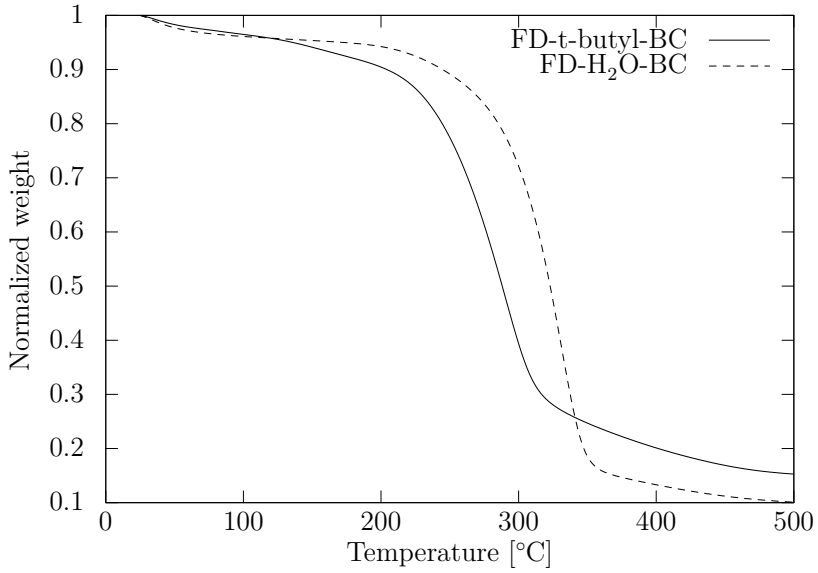

Figure 2.9: TGA plots for freeze-dried BC at a heating rate of 10 °C min^{-1} in an inert atmosphere. Solvent exchange from water to tertiary butyl was done for one of the samples resulting in an earlier degradation onset temperature and better yield.

under various conditions shows a moderate increase in char yield at 350 °C increasing from below 12 % to 22 % [178]. Immersion of cellulose in low concentrated sulfuric acid shows no evidence of chain scission. Sulfate groups are incorporated into the cellulose structure thereby reducing the thermal stability. However the acid environment leads to a reduction in reactive oxygen during pyrolysis increasing the yield. Even more successful results were reported by Kim et al. [179]. They reached yields as high as 38 % after impregnation of cotton in sulfuric acid. They determined the best concentration to be about 6 % H_2SO_4 per dry cellulose. This reduced the shrinkage as well.

Hydrochloric acid was shown to have a similar effect and pyrolysis in an HCl atmosphere also results in a significant increase in carbon residue [140]. Analogous to sulfuric acid, hydrochloric acid dehydrates the cellulose thus reducing the forming of volatile compounds. Residual weight increased from below 10 % to about 25 %.

Increases in carbon yield are also observed by impregnation with ammonium phosphates and sulfates nearly doubling yield compared to untreated material [180].

To try some form of hot-stretching a device made out of graphite was used. It is pictured in figure 2.10. The device head consists of two parts, which are held together via tape. The fibers are loosely wound around the head. During the pyrolysis the tape burns, releasing the lower half of the head which exerts a force on the fibers. However, the tape is incinerated early in the process due to the low thermal stability resulting at least partially in fracture of the fibers during their weakest period, most likely carbonization. If it didn't rip the fibers the weight of the piece proved insufficient to effectively stretch the fibers, at least in the tested conditions. Since no substantial amount of graphitization was reached, the applied force might have just been in vain.

The mechanical properties were not examined in a scientific manner. The poor results of Raman spectroscopy and XRD coupled with the mere fact that a bundle of fibers had a

Figure 2.10: The device that was used to put a load on the fibers during HTT. In this configuration, a dried BC pellicle in tape form and a bundle of LCC fibers were used with the device.

lower strength after pyrolysis discouraged further investigations. Whereas the untreated BC and LCC fibers showed some resistance to being torn apart, the pyrolyzed fibers from either precursor was severely weakened so that handling proved difficult to not crumble the material. This is an indication that the cellulose fibers didn't transform past an amorphous carbon structure during the heat treatment Examination of the pyrolyzed carbon fibers under the SEM didn't reveal any substantial information besides a slight decrease in width. Figure 2.11 shows pyrolyzed BC fibers after HTT of 2200 °C.

2.4 Future research suggestions

With the increasing demand for carbon fibers, there is a possibility of a market for carbon fibers based on sustainable materials. Some of the less explored cellulose materials show

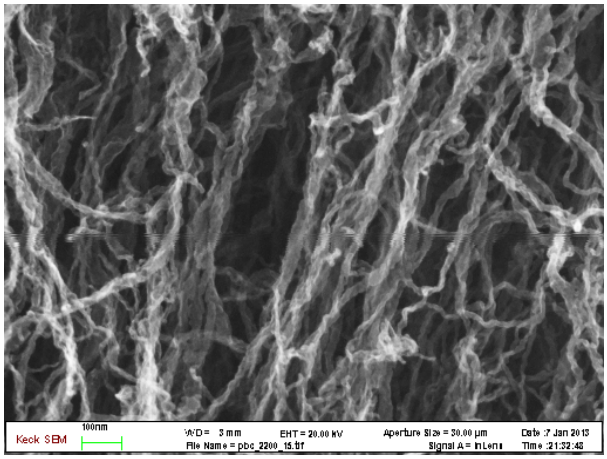

Figure 2.11: Pyrolyzed BC fibers after HTT up to 2200 °C.

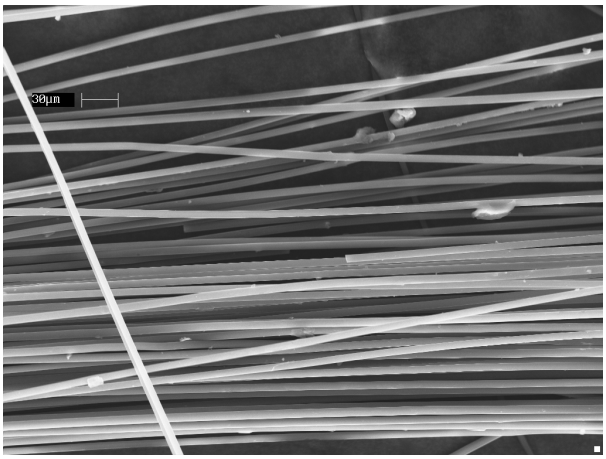

Figure 2.12: Pyrolyzed LCC fibers after HTT up to 2200 °C.

promise to fill that market. Due to their unique structure they might have a different property profile than viscose rayon based CF but share a very similar base structure which provides a good foundation for progress in transforming these materials into carbon fibers.

Technical limitations didn't allow for investigations at temperatures above 2300 °C in the present research. Only at about 2500 °C does graphitization happen much more readily and completely. Generally the higher the heat treatment temperature the larger the degree of graphitization. Cellulose is non-graphitizing, so a turbostratic structure is expected to form at those temperatures. A furnace that at least is able to reach 2800 °C is needed to study the graphitization behavior of BC in a meaningful manner.

An equally important limitation was the inability to do hot-stretching. A large degree of graphitization is only as good as the orientation of the graphitic crystals inside the fibers. This is directly related to the mechanical properties the CF will exhibit. The solution used during the experiments was insufficient to stress the fibers enough especially at high temperatures whereas it tended to break the fibers during the carbonization phase. A system which is able to apply an increased amount of force during the high temperature treatment is adamant to improve the properties of the pyrolyzed BC fibers.

A better carbon yield should also prove to be beneficial to the properties. Maximizing the yield via one of the methods described above would keep the cross-sectional area closer to the untreated fiber and thus reduce the stress on the fibers.

A different approach to heat treating bacterial cellulose in a lab setting which would be interesting to investigate is via electrical current or laser treatment. Both techniques would reduce the need for massively expensive furnaces while allowing for easier stretching during the process.

3 Energy harvesting based on the inherent piezoelectricity of bacterial cellulose

3.1 Introduction

Recent technological developments are rapidly changing the energy landscape in today's world. On one hand, the rapid advancements in miniaturization of individual electronic components bringing with it a decrease in power requirements. The miniaturization promotes an increased deployment of portable systems for personal computing, health and environment monitoring to name a few. These devices pack a lot of capabilities into small packages enabling them to operate autonomously and, in many cases, remotely. Figure 3.1 shows the correlation between the size factor and the diversification of applications and usage scenarios. These so called "smart" systems typically rely on a battery as their power source at the moment.

On the other hand, the realization of the impact of mankind's reliance on fossil fuels on our environment has led to a surge in significantly increased research into sustainable energy sources in the past two decades. Besides the major technologies like photovoltaics,

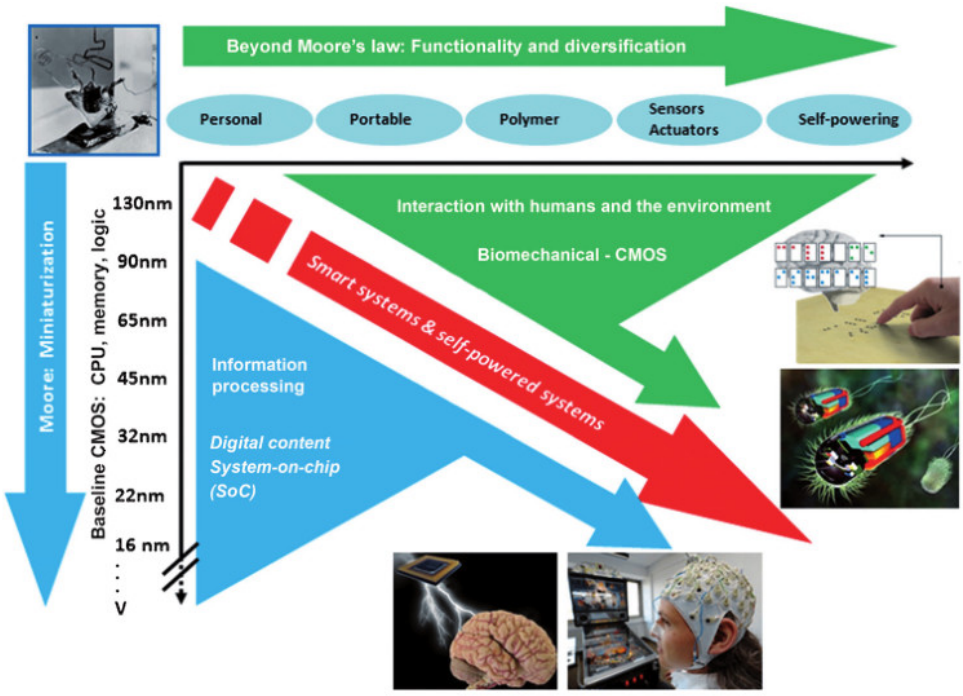

Figure 3.1: The diversification of applications and usage scenarios of portable electronic devices and the increasing miniaturization accompanied by increase in capabilities promotes the developments of smart and self-powered systems [181].

wind turbines and biomass plants, the exploration of other environmental sources has shown a slew of possibilities. While a lot of effort has gone into replacing the primary sources of power on a large scale, the increase in low-power devices mentioned earlier has opened the door for sources to be tapped that seemed insufficient and impractical before.

The prospect of extracting power from abundant chemical and physical sources in the environment has sparked a widespread research effort. A sensor which could draw power from its environment allowing it to operate basically indefinitely without a change of batteries or other human interaction would reduce operational costs and potentially alleviate challenges in waste recycling, pollution and depletion of resources. This trend could lead to the development of small-form factor devices that are self-sustaining and at the same time environmentally friendly. The term energy harvesting is mainly used in this context. In its

most general form it refers to the generation of energy from ambient environmental sources that don't need any form of extraction or generation like coal, gas, oil and nuclear fuel. This includes, among others, solar energy, wind, temperature and concentration gradients, geothermal, kinetic energy and friction. More commonly, however, energy harvesting is used for materials and devices that can harvest energy on a micro-scale. The power output might only be in the milliwatt range, but that would be enough to provide continuous power for a low-power sensor or actuator enabling it to operate independently. This is very critical when such devices are positioned at remote locations that are hard to reach. Most of the mentioned sources are barely exploited as of yet, but they are seemingly infinitely available.

In the same vein an effort to include environmentally sustainable and non-toxic, biocompatible materials into standard devices is taking place. The ongoing depletion of resources increasingly shines a light on the necessity to employ natural materials to replace synthetic ones.

In this section energy harvesting will be explained in more detail as well as some current research examples presented. After that bacterial cellulose and its potential to be used for energy harvesting purposes will be investigated.

3.2 Energy harvesting

Research has looked at multiple different ways to harvest energy, particularly freely available energy. Solar power is extensively researched and is becoming more and more popular in the form of photovoltaics [182, 183, 184] and solar thermal plants [185, 186, 187]. Wind [188] and bio-waste [189] are other commonly used sources with wind parks being set-up which consist of hundreds of wind turbines [190]. Bio-waste plants are also heavily investigated to regain some of the energy used in farming [191]. Further projects look at waves and tidal energy

[192, 193], even though those technologies still have to mature before being commercially viable. All these commonly known "green" sources provide energy at a reasonably large scale and are therefore being developed to provide an alternative to conventional sources and in the future to eventually replace them. What indeed is not often found in the news is the effort to tap microscopic sources that may not produce enough energy to meaningfully contribute to the power grid but may be able to recharge a phone or power a wireless sensor. With the trend and opportunities to provide more and more sensing wirelessly, the question of energy supply is frequently asked. Conventionally, batteries would provide the needed power until they are depleted at which point a replacement or recharging has to happen. This obviously is a disadvantage for devices at remote or hard to reach locations. If a sensor was placed inside the human body during surgery to monitor the healing process the battery basically has to provide enough charge to last the full healing period since a second surgery to replace the battery is not desirable. In any case continuous operation is preferable so that if something unexpected happens the device is still being able to function. Another aspect is size. As devices and sensors get smaller and smaller a battery proves to be a rather bulky add-on due to the size being dependent on the charge density. If the device would integrate sensor, wireless transmitter and energy harvester in one package to allow for continuous operation, a huge step could be taken in the right direction.

Research into the possibility of energy scavenging devices is happening in a multitude of areas. As shown above, of greater interest are thermoelectric materials to exploit thermal gradients [194, 195], microbial fuel cells to exploit the degradation activities of bacteria [196, 197, 198] and pyroelectric materials to benefit from temperature changes [199, 200]. One of the most readily available forms of energy, however, is kinetic energy. Thus harvesting of this kind of energy has enjoyed special attention in recent years. One of the advantages of mechanical energy harvesting is its potential to be applicable on a large scale with

products already available for pavements [201] and ambitious ideas to relieve power crises in third world countries [202]. One possible way to harvest mechanical energy is to use triboelectricity which utilizes charge separation when materials with different chemical potential come in contact [203, 204]. Another method with great potential is piezoelectricity. The piezoelectric effect is well understood and is being used in various applications ranging from automotive injection systems to speakers to cigarette lighters, to name but a few. It compares favorably to other power sources, potentially delivering up to a few hundred milliwatts per cubic centimeter [205].

There are a few examples of the integration energy harvesting techniques into devices. Ramadass and Chandrakasan [206] have fabricated a CMOS circuit to maximize the power extraction from a thermoelectric generator to be worn on the human body. Where previously a battery was needed to start the power extraction, they managed to harvest the energy produced by a thermocouple without any assistance. They are taking advantage of motion by the human body to trigger the charging of the necessary capacitors to jump start the circuit and optimize the power extraction. A typical thermoelectric voltage output is too low to operate CMOS switches to operate a control circuit to enhance the energy stored in a capacitor when being worn. However, Ramadass and Chandrakasan have exploited the fact that their circuit was meant to be wearable and thus subject to constant tiny vibrations due to movement and incorporated a sensitive switch that mechanically triggered the energy storage. With that they were able to create a device that is able to store 58 % of the energy created by the thermoelectric harvester.

Tender et al. [207] used a microbial fuel cell (MFC) to operate a measuring buoy. The bouy transmitted data about water temperature, air pressure, temperature and relative humidity wirelessly. The electronics were powered by the MFC which, in its second generation, produced 36 mW continuously. This is one of the first practical employments of an MFC

showing that the technology is able to reliably produce energy over a long time span. The buoy is a macroscopic tool and the MFC employed by Tender was quite large at a volume of $0.03\,\mathrm{m}^3$. But MFCs have also been demonstrated for use in microscopic applications.

Wang [208] presented a nanowire generator using ZnO. ZnO exhibits piezoelectric properties when shear deformed and is a promising material due to its relative biosafety and availability in several nanostructures like belts, springs and helices, among others. Wang used an AFM tiphead to bend vertically grown nanowires and transduce mechanical energy to electrical energy. Figure 3.2 shows the vertically grown ZnO nanowires and the schematic of the experiment performed. The bending of the nanowire resulted in charge separation across the nanowire. The initial power output of a single wire at resonance was estimated to be around 0.5 pW. Embedding those nanowires into a matrix and optimizing the configuration they were able to create nanogenerators with power output of up to $11\,\mathrm{mW/cm}^3$ and a voltage output of around 2 V [209].

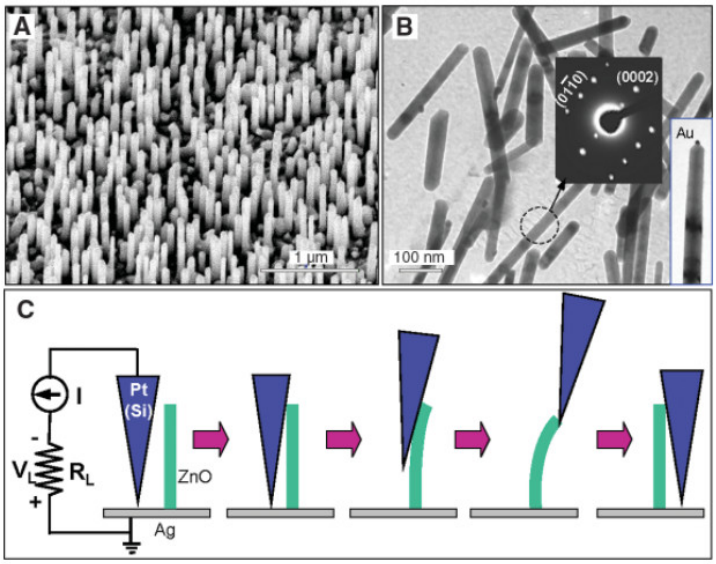

Figure 3.2: An SEM and TEM image of the vertically grown ZnO nanowires are shown in **A** and **B**. **C** shows a schematic of the AFM experiment with a conducting tip [208].

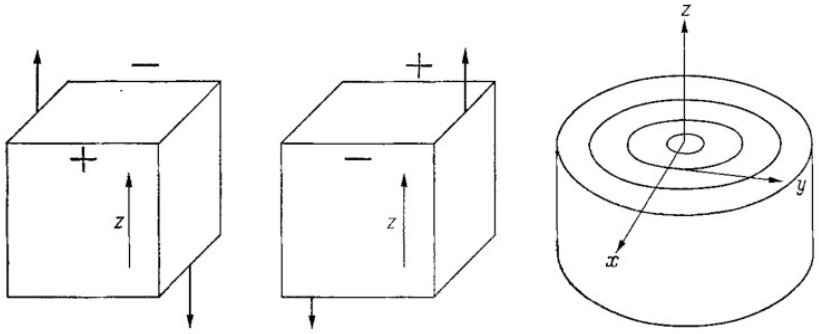

Figure 3.3: Applied shear stress and resulting polarization of rectangular pieces of wood. Grains are aligned in the z-direction and therefore also cellulose crystals [213].

Lead zirconate titanate (PZT) is the best known and most widely used piezoelectric material. However, due to it containing lead, concerns over its effect on health and the environment have been raised and an initiative by the European Union was started to replace it with more environmentally friendly materials where possible [210]. Efforts to find equally suitable materials have not been successful at the time of writing, even though there was a strong push. Alternatives are ZnO, $BaTiO_3$ and electro-active polymers like PVDF. Even though piezoelectricity is a naturally occurring phenomenon there has not been much investigation into natural materials exhibiting piezoelectricity.

3.3 Energy harvesting based on cellulose

3.3.1 Piezoelectricity in cellulosic materials

Cellulose was shown to be piezoelectric in 1955 by Fukada [211]. After Bazhenov and Konstantinova [212] discovered piezoelectricity in wood in 1950, Fukada [211] found that this effect comes from the crystalline parts of cellulose inside the wood macrostructure.

The symmetry of natural cellulose allows for the following piezoelectric tensor [214]:

$$\begin{bmatrix} 0 & 0 & 0 & d_{14} & d_{15} & 0 \\ 0 & 0 & 0 & d_{24} & d_{25} & 0 \\ d_{31} & d_{32} & d_{33} & 0 & 0 & d_{36} \end{bmatrix}$$

The piezoelectric constant d relates the induced polarization D to the stresses T applied to the material, so that $D = dT$ in its simplest form. Fukada [213] theorized that due to the parallel orientation of the cellulose crystals along the grain direction and his findings of polarization only with shear strain applied in the grain direction that cellulose is shear piezoelectric where every constant is zero except d_{14} and d_{25} which are equal in value but opposite as seen in figure 3.3. The piezoelectric tensor of cellulose thus looks as follows:

$$\begin{bmatrix} 0 & 0 & 0 & d_{14} & 0 & 0 \\ 0 & 0 & 0 & 0 & -d_{14} & 0 \\ 0 & 0 & 0 & 0 & 0 & 0 \end{bmatrix}.$$

This results from the monoclinic unit cell structure of the investigated samples as well as the specific configuration of the cellulose. For triclinic unit cell as in the case of cellulose I_β , none of the constants have to be zero [215]. No further investigations into the matter have been reported. As expected piezoelectricity strongly depends on the crystallinity of the materials. A ramie bundle which generally shows high crystallinity of up to 90 % [216] and a rayon bundle with low crystallinity have piezoelectric moduli of about one tenth and one hundredth of quartz, respectively [213]. $d_{14} = 0.2\,\mathrm{pC\,N^{-1}}$ for ramie[217].

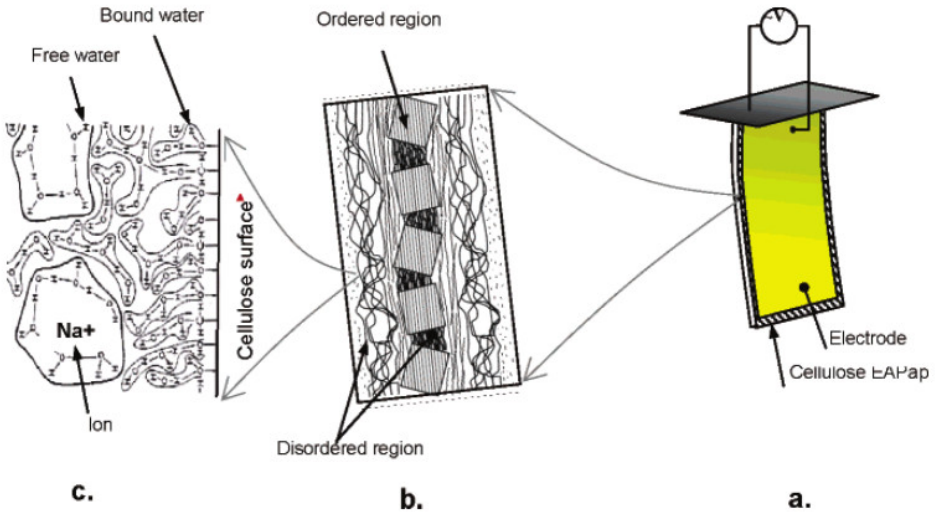

Figure 3.4: Morphology of regenerated cellulose used in EAPap as well as schematic of EAPap cantilever.

3.3.2 Previous research

After the initial discovery the interest in cellulose and its piezoelectricity waned. Few studies were performed, mostly concentrating on wood as a whole [218, 219]. Only in 2006, Kim et al. [220] rediscovered the potential to use cellulose's piezoelectricity in what they called electro-active paper (EAPap). Kim et al. [220] used regenerated cellulose coated with gold to produce what is essentially paper that bends when an electric field is applied across both sides. Similar to piezoelectricity in wood, the preferential alignment of the cellulose molecules along the sheet gives rise to polarization when an electric field is applied orthogonal to the sheet plain resulting in a bending motion. This is the reverse effect of what Bazhenov and Konstantinova [212] and Fukada [211] experienced. Dipole orientation of the hydroxyl groups and incorporated water as well as ion migration are attributed with creating the polarization. The non-centrosymmetric structure of cellulose is inherently piezoelectric and a high concentration of sodium ions is present due to the regeneration of native cellulose in sodium hydroxide.

This EAPap exhibited an activation voltage of around $250\,\mathrm{V\,mm^{-1}}$ and a tip displacement of 4.3 mm was achieved for cantilevers of length of 40 mm [221]. The activation energy is comparable to other electro-active polymers. Kim et al. [222] reported that the piezoelectric charge constant for EAPap is $28.2\,\mathrm{pC\,N^{-1}}$.

This is higher than some of the more widely investigated electro-active polymers such as PVDF. Studying environmental effects on the activation of EAPap, the same group found that with increasing humidity the activation increases [221]. Since cellulose readily absorbs water and the proposed effect of water on the polarization, this isn't too surprising. They also suggest ion migration is considerably easier through water which would explain further increase in displacement. Another factor is the decreasing mechanical properties. In the wet state, the Young's modulus of cellulose decreases [223]. The overall conversion of electrical to mechanical power was not very efficient, being in the range of 0.2 %.

EAPap also constrains in-plane when a voltage is applied, even though this strain is small. With a preferred orientation of 45 degrees of the fibers with respect to the long axis of the cantilever the strain under a constant voltage of 7 V was recorded to be 0.0428 %. Under an alternating voltage of 0.5 Hz the strain reached 0.0373 %. In both cases under a continuous load the contraction reduced gradually over time, i. e. creep under constant conditions causes the cantilevers to elongate again over time.

Thickness as a factor was also investigated [224]. Three different samples with different thicknesses were bent. It was found that the displacement of the cantilever decreased with increasing thickness which can be explained by an increase in bending stiffness. Yun et al. [224] proposed an optimum thickness to achieve the highest efficiency of electrical to mechanical power conversion. According to their data this optimum thickness lies around 30 µm.

In another experiment Yun and Kim [225] mixed 0.1 % multi-walled carbon nanotubes

(MWCNT) into the EAPap to increase the mechanical properties. The cellulose and CNT are dispersed in a solution and then spin cast and pressed on a silicon wafer. The incorporation of nanotubes increases the Young's modulus from 1.02 GPa to 1.80 GPa. As expected, the deflection of the cantilever reduces but the resonance frequency increases so that the mechanical power output rises which means more work can be done.

Wood cellulose was also used in experiments to create electro-active paper [226]. Barium titanate nanoparticles were coated onto the wood fibers. Unlike other paper variants investigated, this resulted in a piezoelectric response when the paper was stretched, not when bent.

Apart from these efforts, actuators on bacterial cellulose were investigated. Kim et al. [227] incorporated different ionic liquids into freeze-dried bacterial cellulose pellicles and coated these with PEDOT:PSS conductive polymer electrodes. The so prepared cantilevers showed displacements at a resonance frequency of 0.1 Hz. The polarization was mainly attributed to ion migration. Similar efforts were done with covalently grafting the carbon nanotubes onto the cellulose fibers [228]. This resulted in an increase in the piezoelectric charge constant. Jeon et al. [229] fabricated a bacterial cellulose actuator that was driven submerged in DI water. The dried BC pellicles were infused with LiCl solution and then electrodes were sputtered onto both sides. The tip displacement improved compared to untreated BC and increased with increasing driving voltage. However, the plant cellulose sample didn't show any bending which was attributed to high water absorption. A comparison of the water uptake of the two celluloses wasn't reported.

In an effort to investigate the energy harvesting potential of EAPap, Zhai et al. [230] investigated the output voltage. They found a response of the EAPap to be from around 50 mV to 150 mV depending on the size and material used. An aluminum electrode resulted in the highest voltage. No explanation for the unusual size dependence was given.

3.4 Bacterial cellulose energy harvesting

Most of the above described investigations looked at either regenerated cellulose or incorporated a different charge carrier into native cellulose, essentially using the cellulose as a very porous and flexible substrate. Furthermore, insight into the direct piezoelectric effect has been basically non-existent except for the very recent one by Zhai et al. [230]. With the increased emphasis on energy related technology the goal for the project resulting in this Master's thesis was to investigate the feasibility and performance of a nanogenerator based on micro-sized bacterial cellulose nanofiber bundles. The reports of the inherent piezoelectricity of native as well as regenerated cellulose showed promise that this could be done. The high crystallinity of bacterial cellulose were thought to be advantageous to the piezoelectric properties.

However, there are mixed results in regards to the piezoelectricity of bacterial cellulose. Kim and Seo [231] didn't see any evidence for piezoelectricity in bacterial cellulose samples during a preliminary investigation into what would eventually become their electro-active paper EAPap. On the other hand, Jeon et al. [229] and Kim et al. [227] saw bending under an electric field to varying degree. Apart from these few reports, there are no publications on the piezoelectricity of bacterial cellulose to the author's knowledge.

Even though, there are unfortunately no quantitative results, the experiments performed in this study confirmed that BC is piezoelectric, as was expected. Unfortunately there's no data to the extent of the piezoelectric constants. The experiment followed those set up by previous publications [231]: a BC rectangular cantilever of dimensions 10 mm x 50 mm coated on both sides with gold electrodes was put under an electric field as seen in figure 3.4. The BC production mirrored the procedure outlined in chapter 1. The thickness of the pellicles was dependent on the days of incubation and the drying method. Profilometry revealed the thickness for oven-dried pellicles to be in the range of a few micrometers and

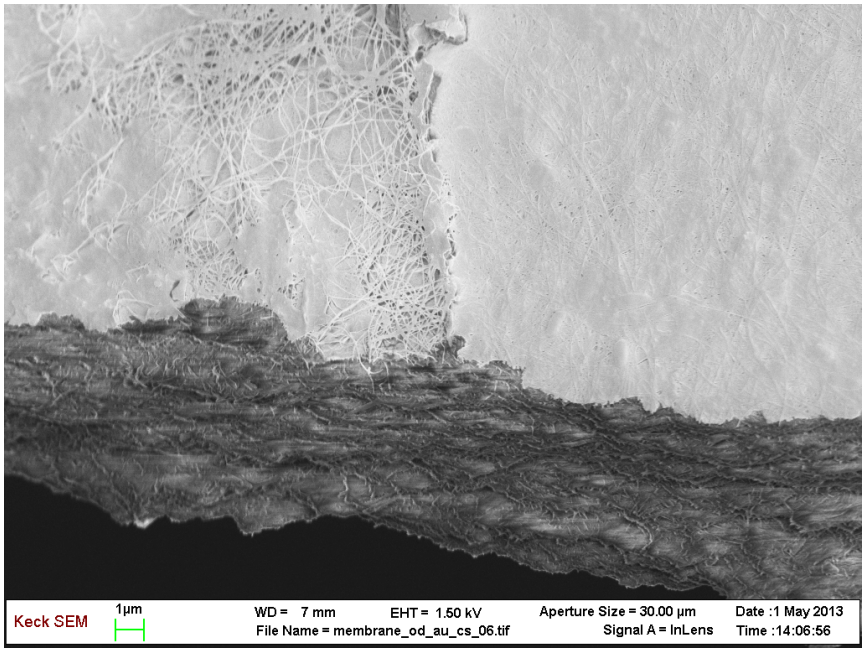

Figure 3.5: Cross-sectional view of a gold coated BC pellicle. On top is a thin gold layer (30 nm). In this image there is no indication that the gold penetrated through the pellicle to connect with the backside.

for freeze-dried BC up to several tenths of micrometers. In general oven-dried samples were used due to large thickness variations across freeze-dried ones. The gold coating was done in a CVC SC4500 evaporator. Gold was chosen because of its environmental stability. Due to the lack of oxidation, there were no problems connecting to the electrodes. The goal for the coating was to affect the stiffness of the BC as little as possible while still providing a continuous layer to allow for uninterrupted current flow.

A good compromise was found at a thickness of 20 nm to 30 nm. The coating was found to be challenging. Even with no apparent cracks or holes, the front and back side of the BC were consistently shorted. Scanning electron microscopy gave no indication that the metal was penetrating all the way through the pores as shown in figure 3.5. Due to the extensive volume loss during drying, micro-fractures are hypothesized to exist in the pellicle allowing the metal coatings to connect. To alleviate that problem micro transfer printing (MTP)

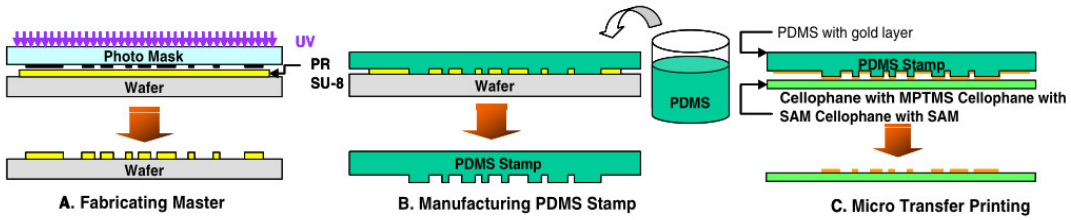

Figure 3.6: Micro transfer printing technique for depositing gold onto cellulose films according to Kim et al. [232].

was tried but was unsuccessful. MTP was previously done on a regenerated cellulose film by Kim et al. [232] as shown in figure 3.6.

Following the reported procedure of using a gold coated PDMS stamp didn't result in a continuous layer. The inherent roughness of the BC pellicle hindered a proper release of the gold layer from the PDMS. As an initial solution a separation layer was put between two BC pellicles.

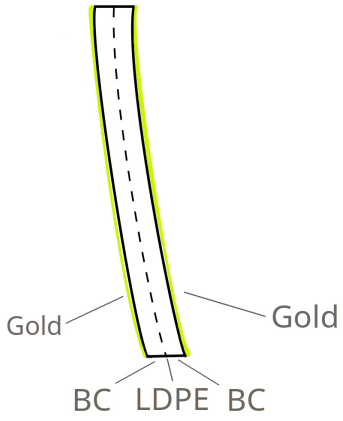

Figure 3.7: A thin LDPE film was sandwiched between two BC pellicles and hot-pressed to prevent shorting of both gold coatings.

The separation layer was very thin LDPE foil that was physically connected to the BC by hot pressing the BC-LDPE-sandwich at around 120 °C, close to the melting temperature of LDPE. The resulting triple-layer, as shown in figure 3.7, could be coated in the evaporator without shorting. Two qualitative observations about the piezoelectric behavior of these

cantilevers were made: the displacement of the tip increased with the applied electric field and was dependent on the frequency of the voltage. The resonant frequency was around 4 Hz to 5 Hz at the given sample size. These observations concur with previously reported behavior of cellulose actuators [220]. As a control sample cellophane was used. Cellophane is a cellulose derivative and was previously used in the actuator experiments [231]. Since it is a cast film, it didn't suffer from the shorting experienced with BC and thus could be coated without any separation layer. The response, however, to an applied electric field was very similar to the BC samples. Even the resonant frequency was in the same range. Frame by frame analysis of videos taken during the experiments revealed a linear relationship between the applied and observed frequencies. This behavior rules out electrostriction as the cause of the oscillations.

The ultimate goal being the investigation of the energy harvesting capabilities of BC on a microscale, membrane like test samples were designed. The vibrations of a membrane, with circular cross-section, are well known and such membranes are regularly used in MEMS characterization [233, 234]. A taut membrane also offers the benefit of increasing the resonant frequency towards regions which can be measured with standard electronic equipment. For preliminary tests, metal washers with inner diameters of a few millimeters were used as substrates. These allowed easy contact to the back side of the membrane. Tests under optical microscopy revealed vibration response for at least one of the membranes under alternating voltage. These membranes, however, suffered from poor handling and they were usually slumping instead of being taut. For further experiments, thin cover glass pieces were utilized. The BC was oven-dried directly on the glass substrate. This had two benefits: excellent adhesion between the substrate and BC and shrinkage during drying ensured that the membrane would be taut. As glass substrates 150 µm thin microscope cover slips were used. Holes of various sizes were laser-drilled into the substrate with a

Versalaser CO_2 laser cutter. The nominal diameter ranged from 1000 µm down to 25 µm. Gold was then evaporated on both sides of the membrane-glass package. The samples were tilted and rotated during processing of the backside to get a uniform coating of the sidewalls of the hole. Electrical connections were put on the system, two in front, two in back, to test the electrical impedance of frontside and backside and ensure that the membrane wasn't shorted from front to back. The package was then glued to a piezoelectric PZT element which worked as the driving actuator. The membrane was suspended over the edge of the PZT to reinforce vibrations. The whole fabrication process is shown in figure 3.8.

The measurements were done using a spectrum analyzer driving the PZT element at 1 mW and sweeping through a range of frequencies. The output signal from the membrane was recorded with the same tool in dB gain. The input and output impedance of the tool was 1 MΩ. Since the impendances of the samples were comparably small, only a couple hundred Ω, this meant that the output power could easily be calculated through the input power and the gain as seen follows:

$$\text{Gain} = 10 \log \left(\frac{P_{out}}{P_{in}} \right) \text{dB}$$

$$P_{out} = P_{in} \exp \left(\frac{Gain}{10} \right)$$

Knowing the impedances, it would have been possible to calculate the output voltage.

Problems executing the measurement successfully were met, however. There was no clear output signal above the background noise in the measurable range of frequencies detected. A variety of issues might have been the cause of this. For some samples it was discovered that the electrical connection across the sidewall was poor or broken. Even the tilting and rotating of the samples during evaporation wasn't enough to get uniform coverage of the sidewalls. The resonant frequency of the membrane might still have been too low

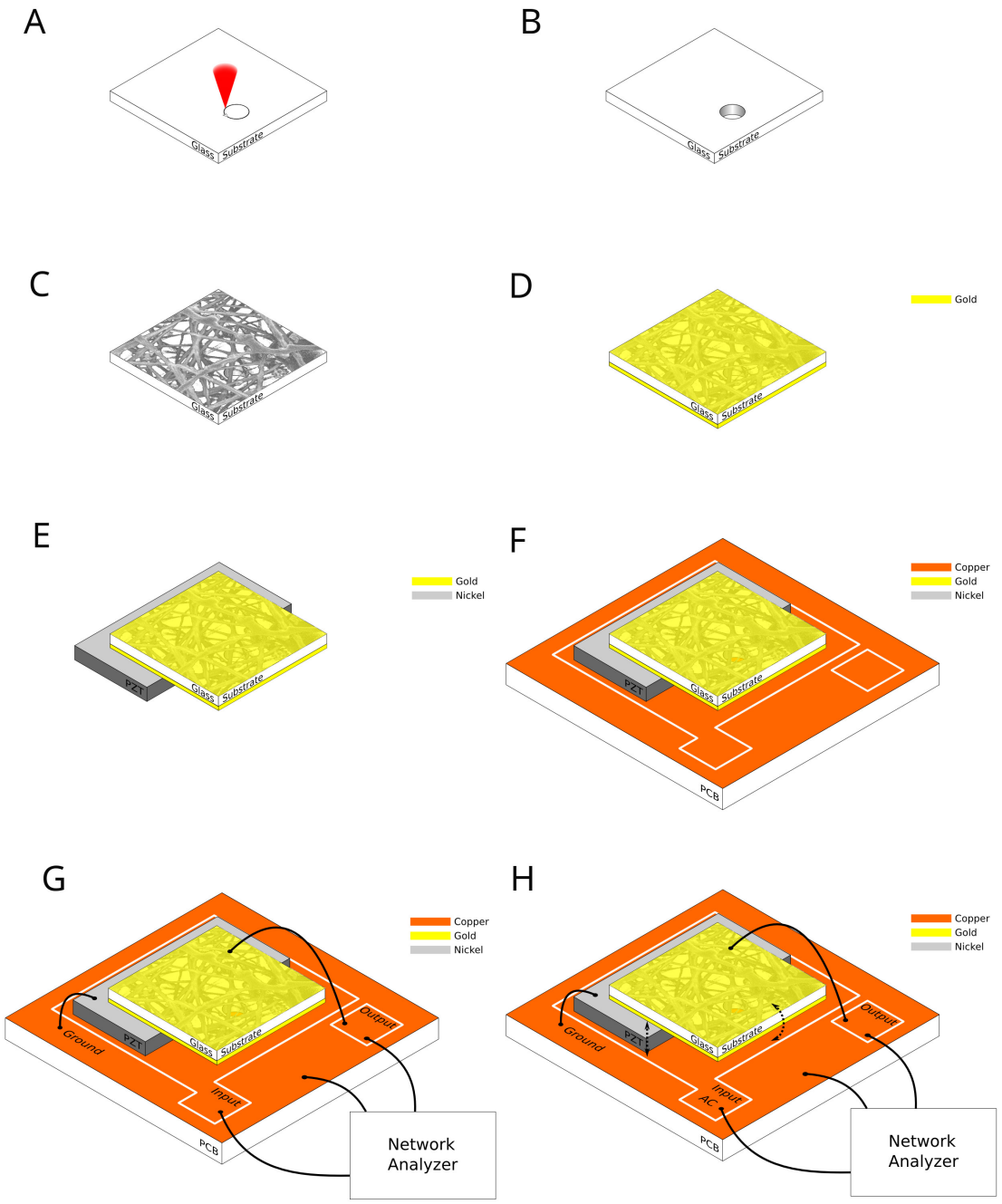

Figure 3.8: The membrane sample fabrication process. **A**, **B** Laser cutting of the substrate; **C** Depositing and drying of BC; **D** Gold evaporation on front and backside; **E** Packages is glued onto PZT with Nickel electrodes; **F** Assembly of package onto a copper-clad PCB board; **G** Soldering of wires to connect to network analyzer. **H** Resulting output. For more detail, see paragraph on page 62.

and therefore outside of the measured range. The utilized PZT elements had a resonant frequency of about 7 kHz. Furthermore the spectrum analyzer had a lower limit of 1 kHz. Given that the pellicle as a whole is not very stiff, the tension in the membrane might not have been enough to elevate the resonant frequency above the lower threshold. On the other hand, the amplitude of a very stiff membrane is small. The expected low piezoelectric response in addition to a low amplitude might have resulted in a very low signal which could not have been detected above the background noise.

3.5 Future research

Quantitative analysis is necessary to judge the feasibility of a bacterial cellulose based nanogenerator. This should be the primary focus of any future research in this area. There is no clear indication of any potential without quantitative results.

Meant as a temporary solution, the BC-LDPE sandwich unnecessarily increases the stiffness of the cantilever. The removal of the LDPE separation layer can be achieved by successfully applying the proposed micro transfer printing method. Another solution might be to increase the thickness of the BC pellicles, even though this approach has its limitations.

A very important aspect to the piezoelectric performance of cellulose is the alignment of the fibers. Generally BC is randomly oriented in the plane of the pellicle. Thus only a fraction of the fibers actually contribute towards the piezoresponse. However, implementing the methods outlined in chapter 1 to force a more uniform alignment could potentially lead to a vast improvement in the piezoelectric performance. It should also be possible to stretch, possibly in wet condition, the BC yarn to improve the orientation. It has been reported that a 45° angle of the fibers to the bending motion results in the biggest response.

In the end, most importantly, a different approach to measuring the power output of a

BC device needs to be chosen. A system with more known parameters would be a good first start. An idea was to use an AFM tip as a substrate which can be chosen and characterized as to its deflection and frequency. This would have the benefit of a simplified fabrication and less problems connecting to the device.

In terms of fabricating a cantilever, the problems lie in the target size. A cantilever on the microscale is difficult to produce due to handling and coating issues. A cantilever of that size is very fragile and depositing electrodes on either side is going to be a challenge.

References

[1] A. O'Sullivan. "Cellulose: the structure slowly unravels". *Cellulose* 4(3), 1997, pp. 173–207.

[2] D. Klemm, B. Heublein, H.-P. Fink, and A. Bohn. "Cellulose: Fascinating Biopolymer and Sustainable Raw Material". *Angewandte Chemie International Edition* 44(22), 2005, pp. 3358–3393.

[3] K. Qiu and A. N. Netravali. "Bacterial cellulose-based membrane-like biodegradable composites using cross-linked and noncross-linked polyvinyl alcohol". *J Mater Sci* 47(16), 2012, pp. 6066–6075.

[4] D. Klemm, D. Schumann, U. Udhardt, and S. Marsch. "Bacterial synthesized cellulose —artificial blood vessels for microsurgery". *Prog Polym Sci* 26(9), 2001, pp. 1561–1603.

[5] A. J. Brown. "XLIII.—On an acetic ferment which forms cellulose". *Journal of the Chemical Society, Transactions* 49, 1886, pp. 432–439.

[6] W. Zopf. *Die Spaltpilze*. Eduard Trewendt, 1885.

[7] S. Thomson. "Notes on the Vinegar-Plant". *Association medical journal* 1(36), 1853, p. 789.

[8] F. Kützing. "Microscopische Untersuchungen über die Hefe und Essigmutter, nebst mehreren andern dazu gehörigen vegetabilischen Gebilden". *Journal für praktische Chemie* 11(1), 1837, pp. 385–409.

[9] Y. Yamada, K.-i. Hoshino, and T. Ishikawa. "The Phylogeny of Acetic Acid Bacteria Based on the Partial Sequences of 16S Ribosomal RNA : The Elevation of the Subgenus Gluconoacetobacter to the Generic Level". *Biosci. Biotechnol. Biochem.* 61(8), 1997, pp. 1244–1251.

[10] "Validation list no. 64: Validation of publication of new names and new combinations previously effectively published outside the IJSB". *International Journal of Systematic Biology* 48(1), 1998, pp. 327–328.

[11] M. M. Lapuz, E. G. Gallardo, and M. A. Palo. "The nata organism: cultural requirements, characteristics and identity". *Philippine Journal of Science* 96(2), 1967, pp. 91–111.

[12] Eliane Trovatti. "The future of bacterial cellulose and other microbial polysaccharides". *Journal of Renewable Materials* 1(1), 2013, pp. 28–41.

[13] A. Payen. "Mémoire sur la composition du tissu propre des plantes et du ligneux". *Comptes rendus* 7, 1838, pp. 1052–1056.

[14] J. Dumas. "Rapport fait à l'Académie des Sciences, dans sa séance du 2 janvier 1839, sur un mémoire de M. Payen, relatif à la composition de la matière ligneuse, par M. J. Dumas". *Annales des sciences naturelles*. 2nd ser. 11, 1839, pp. 28–31.

[15] W. N. Haworth. “The structure of carbohydrates”. *Helv Chim Acta* 11(1), 1928, pp. 534–548.

[16] H. Staudinger and K. Feuerstein. “Über hochpolymere Verbindungen. 147. Mitteilung. Über den Polymerisationsgrad natürlicher und technischer Cellulosen”. *Liebigs Ann Chem* 526(1), 1936, pp. 72–102.

[17] E. Sjöström. *Wood Chemistry: Fundamentals and Applications*. Gulf Professional Publishing, 1993.

[18] K. Watanabe, M. Tabuchi, Y. Morinaga, and F. Yoshinaga. “Structural features and properties of bacterial cellulose produced in agitated culture”. *Cellulose* 5(3), 1998, pp. 187–200.

[19] N. Tahara, M. Tabuchi, K. Watanabe, H. Yano, Y. Morinaga, and F. Yoshinaga. “Degree of Polymerization of Cellulose from Acetobacter xylinum BPR2001 Decreased by Cellulase Produced by the Strain”. *Biosci. Biotechnol. Biochem.* 61(11), 1997, pp. 1862–1865.

[20] L. R. Lynd, P. J. Weimer, W. H. v. Zyl, and I. S. Pretorius. “Microbial Cellulose Utilization: Fundamentals and Biotechnology”. *Microbiol Mol Biol R* 66(3), 2002, pp. 506–577.

[21] K. H. Meyer and H. Mark. “Über den Bau des krystallisierten Anteil der Cellulose”. *Ber Dtsch Chem Ges.* B 61(4), 1928, pp. 593–614.

[22] F. T. Peirce. “The mechanism of growth in the cotton hair”. *Trans. Faraday Soc.* 26, 1930, pp. 809–813.

[23] H.-P. Fink, D. Hofmann, and B. Philipp. “Some aspects of lateral chain order in cellulosics from X-ray scattering”. *Cellulose* 2(1), 1995, pp. 51–70.

[24] A. K. Kulshreshtha and N. E. Dweltz. “Paracrystalline lattice disorder in cellulose. I. Reappraisal of the application of the two-phase hypothesis to the analysis of powder x-ray diffractograms of native and hydrolyzed cellulosic materials”. *Journal of Polymer Science: Polymer Physics Edition* 11(3), 1973, pp. 487–497.

[25] S. Park, J. O. Baker, M. E. Himmel, P. A. Parilla, and D. K. Johnson. “Research Cellulose crystallinity index: measurement techniques and their impact on interpreting cellulase performance”. *Biotechnol. Biofuels* 3, 2010, pp. 1–10.

[26] S. Pérez and D. Samain. “Structure and Engineering of Celluloses”. *Advances in Carbohydrate Chemistry and Biochemistry*. Vol. 64. Elsevier, 2010, pp. 25–116.

[27] R. Bacon and M. M. Tang. “Carbonization of cellulose fibers—II. Physical property study”. *Carbon* 2(3), 1964, pp. 221–225.

[28] R. H. Atalla and D. L. Vanderhart. “Native Cellulose: A Composite of Two Distinct Crystalline Forms”. *Int S Techn Pol Inn* 223(4633), 1984, pp. 283–285.

[29] H. Yamamoto and F. Horn. “In Situ crystallization of bacterial cellulose I. Influences of polymeric additives, stirring and temperature on the formation celluloses I α and I β as revealed by cross polarization/magic angle spinning (CP/MAS) 13C NMR spectroscopy”. *Cellulose* 1(1), 1994, pp. 57–66.

[30] S. Kuga and M. Brown Jr. “Silver labeling of the reducing ends of bacterial cellulose”. *Carbohyd Res* 180(2), 1988, pp. 345–350.

[31] F. J. Kolpak and J. Blackwell. “Determination of the Structure of Cellulose II”. *Macromolecules* 9(2), 1976, pp. 273–278.

[32] P. Ross, R. Mayer, and M. Benziman. “Cellulose biosynthesis and function in bacteria.” *Microbiol Rev* 55(1), 1991, pp. 35–58.

[33] M. H. Deinema and L. P. T. M. Zevenhuizen. “Formation of cellulose fibrils by gram-negative bacteria and their role in bacterial flocculation”. *Archiv für Mikrobiologie* 78(1), 1971, pp. 42–57.

[34] K. Matsushita, H. Toyama, and O. Adachi. “Respiratory chains and bioenergetics of acetic acid bacteria”. *Advances in Microbial Physiology*. Academic Press, 1994, pp. 249–301.

[35] *Microbial cellulose. Wikipedia, the free encyclopedia*. 2013.

[36] R. M. Brown, J. H. Willison, and C. L. Richardson. “Cellulose biosynthesis in Acetobacter xylinum: visualization of the site of synthesis and direct measurement of the in vivo process”. *Proceedings of the National Academy of Sciences* 73(12), 1976, pp. 4565–4569.

[37] R. Jonas and L. F. Farah. “Production and application of microbial cellulose”. *Polym Degrad Stabil* 59(1–3), 1998, pp. 101–106.

[38] M. Schramm and S. Hestrin. “Factors affecting production of cellulose at the air/liquid interface of a culture of Acetobacter xylinum”. *J Gen Microbiol* 11(1), 1954, pp. 123–129.

[39] M. E. Embuscado, J. S. Marks, and J. N. Bemiller. “Bacterial cellulose. I. Factors affecting the production of cellulose by Acetobacter xylinum”. *Food Hydrocolloid* 8(5), 1994, pp. 407–418.

[40] K. Sattler and S. Fiedler. “Gewinnung und anwendung von Bakteriencellulose: II. Kultivierung im rotierenden Walzenfermenter”. *Zentralblatt für Mikrobiologie* 145(4), 1990, pp. 247–252.

[41] H.-J. Son, M.-S. Heo, Y.-G. Kim, and S.-J. Lee. “Optimization of fermentation conditions for the production of bacterial cellulose by a newly isolated Acetobacter”. *Biotechnol Appl Bioc* 33(1), 2001, pp. 1–5.

[42] J. W. Hwang, Y. K. Yang, J. K. Hwang, Y. R. Pyun, and Y. S. Kim. “Effects of pH and dissolved oxygen on cellulose production by Acetobacter xylinum BRC5 in agitated culture”. *J Biosci Bioeng* 88(2), 1999, pp. 183–188.

[43] T. Kouda, T. Naritomi, H. Yano, and F. Yoshinaga. “Effects of oxygen and carbon dioxide pressures on bacterial cellulose production by Acetobacter in aerated and agitated culture”. *J Ferment Bioeng* 84(2), 1997, pp. 124–127.

[44] H. Toyosaki, T. Naritomi, A. Seto, M. Matsuoka, T. Tsuchida, and F. Yoshinaga. “Screening of Bacterial Cellulose-producing Acetobacter Strains Suitable for Agitated Culture”. *Biosci. Biotechnol. Biochem.* 59(8), 1995, pp. 1498–1502.

[45] W. Czaja, D. Romanovicz, and R. m. Brown. “Structural investigations of microbial cellulose produced in stationary and agitated culture”. *Cellulose* 11(3-4), 2004, pp. 403–411.

[46] M. Shoda and Y. Sugano. “Recent advances in bacterial cellulose production”. *Biotechnol Bioproc E* 10(1), 2005, pp. 1–8.

[47] A. Sani and Y. Dahman. “Improvements in the production of bacterial synthesized biocellulose nanofibres using different culture methods”. *J Chem Technol Biot* 85(2), 2010, pp. 151–164.

[48] M. E. Embuscado, J. S. Marks, and J. N. Bemiller. “Bacterial cellulose. II. Optimization of cellulose production by Acetobacter xylinum through response surface methodology”. *Food Hydrocolloid* 8(5), 1994, pp. 419–430.

[49] S. Masaoka, T. Ohe, and N. Sakota. “Production of cellulose from glucose by Acetobacter xylinum”. *J Ferment Bioeng* 75(1), 1993, pp. 18–22.

[50] T. Oikawa, T. Morino, and M. Ameyama. “Production of cellulose from D-arabitol by Acetobacter xylinum KU-1”. *Biosci. Biotechnol. Biochem.* 59(8), 1995, pp. 1564–1565.

[51] T. Oikawa, T. Ohtori, and M. Ameyama. “Production of cellulose from D-mannitol by Acetobacter xylinum KU-1”. *Biosci. Biotechnol. Biochem.* 59(2), 1995, pp. 331–332.

[52] F. Hong and K. Qiu. “An alternative carbon source from konjac powder for enhancing production of bacterial cellulose in static cultures by a model strain Acetobacter aceti subsp. xylinus ATCC 23770”. *Carbohyd Polym* 72(3), 2008, pp. 545–549.

[53] K. Qiu and A. N. Netravali. “"Green" composites based on bacterial cellulose produced using novel low-cost carbon source and soy protein resin”. *Recent Advances in Adhesion Science and Technology in Honor of Dr. Kash Mittal*. Ed. by W. V. Gutowski and H. Dodiuk. CRC Press, 2013. Chap. 11, pp. 193–208.

[54] S. Kongruang. “Bacterial Cellulose Production by Acetobacter xylinum Strains from Agricultural Waste Products”. *Appl Biochem Biotech* 148(1-3), 2008, pp. 245–256.

[55] A. N. Netravali and K. Qiu. “Bacterial cellulose based ’green’ composites”. 8,541,001. A. N. Netravali and K. Qiu. 2013.

[56] D. R. Ruka, G. P. Simon, and K. M. Dean. “Altering the growth conditions of Gluconacetobacter xylinus to maximize the yield of bacterial cellulose”. *Carbohyd Polym* 89(2), 2012, pp. 613–622.

[57] K. Watanabe and S. Yamanaka. “Effects of oxygen tension in the gaseous phase on production and physical properties of bacterial cellulose formed under static culture conditions”. *Biosciences Biotechnology and Biochemistry* 59(1), 1995, pp. 65–68.

[58] A. Krystynowicz, W. Czaja, A. Wiktorowska-Jezierska, M. Gonçalves-Miśkiewicz, M. Turkiewicz, and S. Bielecki. “Factors affecting the yield and properties of bacterial cellulose”. *J. Ind. Microbiol. Biotechnol.* 29(4), 2002, pp. 189–195.

[59] D. Mikkelsen, B. Flanagan, G. Dykes, and M. Gidley. “Influence of different carbon sources on bacterial cellulose production by Gluconacetobacter xylinus strain ATCC 53524”. *J Appl Microbiol* 107(2), 2009, pp. 576–583.

[60] H. El-Saied, A. I. El-Diwany, A. H. Basta, N. A. Atwa, and D. E. El-Ghwas. “Production and characterization of economical bacterial cellulose”. *Bioresources* 3(4), 2008, pp. 1196–1217.

[61] B. A. McKenna, D. Mikkelsen, J. B. Wehr, M. J. Gidley, and N. W. Menzies. "Mechanical and structural properties of native and alkali-treated bacterial cellulose produced by Gluconacetobacter xylinus strain ATCC 53524". *Cellulose* 16(6), 2009, pp. 1047–1055.

[62] S. Hesse and T. Kondo. "Behavior of cellulose production of Acetobacter xylinum in 13C-enriched cultivation media including movements on nematic ordered cellulose templates". *Carbohyd Polym* 60(4), 2005, pp. 457–465.

[63] Y. Tomita and T. Kondo. "Influential factors to enhance the moving rate of Acetobacter xylinum due to its nanofiber secretion on oriented templates". *Carbohyd Polym* 77(4), 2009, pp. 754–759.

[64] T. Kondo, M. Nojiri, Y. Hishikawa, E. Togawa, D. Romanovicz, and R. M. Brown. "Biodirected epitaxial nanodeposition of polymers on oriented macromolecular templates". *Proceedings of the National Academy of Sciences* 99(22), 2002, pp. 14008–14013.

[65] M. B. Sano, A. D. Rojas, P. Gatenholm, and R. V. Davalos. "Electromagnetically Controlled Biological Assembly of Aligned Bacterial Cellulose Nanofibers". *Ann Biomed Eng* 38(8), 2010, pp. 2475–2484.

[66] Hugh O'Neill, Barbara Evans, Gary A. Baker, and Roberto Benson. *Directed Biosynthesis of Oriented Crystalline Cellulose for Advanced Composite Fibers*. Final PTS 34511. Oak Ridge, Tennessee: Oak Ridge National Laboratory, 2011, p. 30.

[67] A. Putra, A. Kakugo, H. Furukawa, and J. P. Gong. "Orientated Bacterial Cellulose Culture Controlled by Liquid Substrate of Silicone Oil with Different Viscosity and Thickness". *Polym J* 41(9), 2009, pp. 764–770.

[68] A. Putra, A. Kakugo, H. Furukawa, J. P. Gong, Y. Osada, T. Uemura, and M. Yamamoto. "Production of Bacterial Cellulose with Well Oriented Fibril on PDMS Substrate". *Polym J* 40(2), 2007, pp. 137–142.

[69] A. Putra, A. Kakugo, H. Furukawa, J. P. Gong, and Y. Osada. "Tubular bacterial cellulose gel with oriented fibrils on the curved surface". *Polymer* 49(7), 2008, pp. 1885–1891.

[70] N. Sakairi, H. Asano, M. Ogawa, N. Nishi, and S. Tokura. "A method for direct harvest of bacterial cellulose filaments during continuous cultivation of Acetobacter xylinum". *Carbohyd Polym* 35(3-4), 1998, pp. 233–237.

[71] S. Tokura, H. Asano, N. Sakairi, and N. Nishi. "Direct filature of bacterial cellulose from culture medium". *Macromol Symp* 127(1), 1998, pp. 23–30.

[72] A. Hirai, M. Tsuji, and F. Horii. "Communication: culture conditions producing structure entities composed of cellulose i and ii in bacterial". *Cellulose* 4(3), 1997, pp. 239–245.

[73] A. Budhiono, B. Rosidi, H. Taher, and M. Iguchi. "Kinetic aspects of bacterial cellulose formation in nata-de-coco culture system". *Carbohyd Polym* 40(2), 1999, pp. 137–143.

[74] W. Tang, S. Jia, Y. Jia, and H. Yang. "The influence of fermentation conditions and post-treatment methods on porosity of bacterial cellulose membrane". *World Journal of Microbiology and Biotechnology* 26(1), 2010, pp. 125–131.

[75] R. T. Olsson, M. A. S. Azizi Samir, G. Salazar-Alvarez, L. Belova, V. Ström, L. A. Berglund, O. Ikkala, J. Nogués, and U. W. Gedde. "Making flexible magnetic aerogels and stiff magnetic nanopaper using cellulose nanofibrils as templates". *Nat Nanotechnol* 5(8), 2010, pp. 584–588.

[76] H. Jin, Y. Nishiyama, M. Wada, and S. Kuga. "Nanofibrillar cellulose aerogels". *Colloids and Surfaces A: Physicochemical and Engineering Aspects* 240(1-3), 2004, pp. 63–67.

[77] S. Kuga, D. Kim, Y. Nishiyama, and R. Brown. "Nanofibrillar carbon from native cellulose". *Mol Cryst Liq Cryst* 387(1), 2002, pp. 13–19.

[78] F. Liebner, E. Haimer, M. Wendland, M.-A. Neouze, K. Schlufter, P. Miethe, T. Heinze, A. Potthast, and T. Rosenau. "Aerogels from Unaltered Bacterial Cellulose: Application of scCO2 Drying for the Preparation of Shaped, Ultra-Lightweight Cellulosic Aerogels". *Macromol Biosci* 10(4), 2010, pp. 349–352.

[79] J. Gassan and A. K. Bledzki. "Alkali treatment of jute fibers: Relationship between structure and mechanical properties". *J Appl Polym Sci* 71(4), 1999, pp. 623–629.

[80] K. E. Cabradilla and S. H. Zeronian. "Factors influencing the tensile properties of ramie". *J Appl Polym Sci* 19(2), 1975, pp. 503–517.

[81] Takashi Nishino, Kiyofumi Takano, and Katsuhiko Nakamae. "Elastic Modulus of the Crystalline Regions of Cellulose Polymorphs". *Journal of Polymer Science: Part B: Polymer Physics* 33, 1995, pp. 1647–1651.

[82] G. Guhados, W. Wan, and J. L. Hutter. "Measurement of the Elastic Modulus of Single Bacterial Cellulose Fibers Using Atomic Force Microscopy". *Langmuir* 21(14), 2005, pp. 6642–6646.

[83] Y.-C. Hsieh, H. Yano, M. Nogi, and S. J. Eichhorn. "An estimation of the Young's modulus of bacterial cellulose filaments". *Cellulose* 15(4), 2008, pp. 507–513.

[84] S. J. Eichhorn and R. J. Young. "The Young's modulus of a microcrystalline cellulose". *Cellulose* 8(3), 2001, pp. 197–207.

[85] S. Yamanaka, K. Watanabe, N. Kitamura, M. Iguchi, S. Mitsuhashi, Y. Nishi, and M. Uryu. "The structure and mechanical properties of sheets prepared from bacterial cellulose". *J Mater Sci* 24(9), 1989, pp. 3141–3145.

[86] Y. Nishi, M. Uryu, S. Yamanaka, K. Watanabe, N. Kitamura, M. Iguchi, and S. Mitsuhashi. "The structure and mechanical properties of sheets prepared from bacterial cellulose". *J Mater Sci* 25(6), 1990, pp. 2997–3001.

[87] Y. Hagiwara, A. Putra, A. Kakugo, H. Furukawa, and J. P. Gong. "Ligament-like tough double-network hydrogel based on bacterial". *Cellulose* 17(1), 2010, pp. 93–101.

[88] H. Bäckdahl, G. Helenius, A. Bodin, U. Nannmark, B. R. Johansson, B. Risberg, and P. Gatenholm. "Mechanical properties of bacterial cellulose and interactions with smooth muscle cells". *Biomaterials* 27(9), 2006, pp. 2141–2149.

[89] A. Nakayama, A. Kakugo, J. P. Gong, Y. Osada, M. Takai, T. Erata, and S. Kawano. "High Mechanical Strength Double-Network Hydrogel with Bacterial Cellulose". *Adv Funct Mater* 14(11), 2004, pp. 1124–1128.

[90] C. Clasen, B. Sultanova, T. Wilhelms, P. Heisig, and W.-M. Kulicke. “Effects of Different Drying Processes on the Material Properties of Bacterial Cellulose Membranes”. *Macromol Symp* 244(1), 2006, pp. 48–58.

[91] A. K. Bledzki and J. Gassan. “Composites reinforced with cellulose based fibres”. *Prog Polym Sci* 24(2), 1999, pp. 221–274.

[92] T. Miyamoto, S.-i. Takahashi, H. Ito, H. Inagaki, and Y. Noishiki. “Tissue biocompatibility of cellulose and its derivatives”. *J Biomed Mater Res* 23(1), 1989, pp. 125–133.

[93] G. Helenius, H. Bäckdahl, A. Bodin, U. Nannmark, P. Gatenholm, and B. Risberg. “In vivo biocompatibility of bacterial cellulose”. *J Biomed Mater Res A* 76A(2), 2006, pp. 431–438.

[94] V. T. Nguyen, B. Flanagan, M. J. Gidley, and G. A. Dykes. “Characterization of Cellulose Production by a Gluconacetobacter xylinus Strain from Kombucha”. *Curr Microbiol* 57(5), 2008, pp. 449–453.

[95] A. Okiyama, M. Motoki, and S. Yamanaka. “Bacterial cellulose IV. Application to processed foods”. *Food Hydrocolloid* 6(6), 1993, pp. 503–511.

[96] “Bacterial cellulose-containing molding material having high dynamic strength”. 4742164. M. Iguchi, S. Mitsuhashi, K. Ichimura, Y. Nishi, M. Uryu, S. Yamanaka, and K. Watanabe. 1988.

[97] R. M. Brown. “Microbial cellulose: a new resource for wood, paper, textiles, food and specialty products”. *Position Paper, University of Texas at Austin, Austin, Texas* 1998.

[98] *Biocellulose and Its Use In Headphones-Earphones (referring the recent iem example: Vsonic GR-07 (R07)*. Head-Fi.org. 2011. URL: `/t/568694/biocellulose-and-its-use-in-headphones-earphones-referring-the-recent-iem-example-vsonic-gr-07-r07` (visited on 2014).

[99] *Research and Markets: Global Carbon Fiber Market 2012-2016: Impact of Drivers and Challenges | Business Wire*. 2014. URL: `http://www.businesswire.com/news/home/20140203006039/en/Research-Markets-Global-Carbon-Fiber-Market-2012-2016` (visited on 02/21/2014).

[100] R. A. Pértile, S. Moreira, R. M. Gil da Costa, A. Correia, L. Guãrdao, F. Gartner, M. Vilanova, and M. Gama. “Bacterial Cellulose: Long-Term Biocompatibility Studies”. *J. Biomater. Sci. Polym. Ed.* 23(10), 2012, pp. 1–16.

[101] N. Petersen and P. Gatenholm. “Bacterial cellulose-based materials and medical devices: current state and perspectives”. *Appl Microbiol Biot* 91(5), 2011, pp. 1277–1286.

[102] J. D. Fontana, A. M. De Souza, C. K. Fontana, I. L. Torriani, J. C. Moreschi, B. J. Gallotti, S. J. De Souza, G. P. Narcisco, J. A. Bichara, and L. F. X. Farah. “Acetobacter cellulose pellicle as a temporary skin substitute”. *Appl Biochem Biotech* 24(1), 1990, pp. 253–264.

[103] W. K. Czaja, D. J. Young, M. Kawecki, and R. M. Brown. “The Future Prospects of Microbial Cellulose in Biomedical Applications”. *Biomacromolecules* 8(1), 2007, pp. 1–12.

[104] A. Svensson, E. Nicklasson, T. Harrah, B. Panilaitis, D. L. Kaplan, M. Brittberg, and P. Gatenholm. “Bacterial cellulose as a potential scaffold for tissue engineering of cartilage”. *Biomaterials* 26(4), 2005, pp. 419–431.

[105] Y. Z. Wan, L. Hong, S. R. Jia, Y. Huang, Y. Zhu, Y. L. Wang, and H. J. Jiang. "Synthesis and characterization of hydroxyapatite–bacterial cellulose nanocomposites". *Compos Sci Technol* 66(11–12), 2006, pp. 1825–1832.

[106] M. Zaborowska, A. Bodin, H. Bäckdahl, J. Popp, A. Goldstein, and P. Gatenholm. "Microporous bacterial cellulose as a potential scaffold for bone regeneration". *Acta Biomater* 6(7), 2010, pp. 2540–2547.

[107] V. Favier, H. Chanzy, and J. Y. Cavaille. "Polymer nanocomposites reinforced by cellulose whiskers". *Macromolecules* 28(18), 1995, pp. 6365–6367.

[108] M. Pommet, J. Juntaro, J. Y. Y. Heng, A. Mantalaris, A. F. Lee, K. Wilson, G. Kalinka, M. S. P. Shaffer, and A. Bismarck. "Surface Modification of Natural Fibers Using Bacteria: Depositing Bacterial Cellulose onto Natural Fibers To Create Hierarchical Fiber Reinforced Nanocomposites". *Biomacromolecules* 9(6), 2008, pp. 1643–1651.

[109] J. Juntaro, M. Pommet, G. Kalinka, A. Mantalaris, M. S. P. Shaffer, and A. Bismarck. "Creating Hierarchical Structures in Renewable Composites by Attaching Bacterial Cellulose onto Sisal Fibers". *Adv Mater* 20(16), 2008, pp. 3122–3126.

[110] A. Nakagaito, S. Iwamoto, and H. Yano. "Bacterial cellulose: the ultimate nano-scalar cellulose morphology for the production of high-strength composites". *Applied Physics A* 80(1), 2004, pp. 93–97.

[111] H. Yano, J. Sugiyama, A. N. Nakagaito, M. Nogi, T. Matsuura, M. Hikita, and K. Handa. "Optically Transparent Composites Reinforced with Networks of Bacterial Nanofibers". *Adv Mater* 17(2), 2005, pp. 153–155.

[112] S. C. M. Fernandes, L. Oliveira, C. S. R. Freire, A. J. D. Silvestre, C. P. Neto, A. Gandini, and J. Desbriéres. "Novel transparent nanocomposite films based on chitosan and bacterial cellulose". *Green Chem* 11(12), 2009, pp. 2023–2029.

[113] I. M. G. Martins, S. P. Magina, L. Oliveira, C. S. R. Freire, A. J. D. Silvestre, C. P. Neto, and A. Gandini. "New biocomposites based on thermoplastic starch and bacterial cellulose". *Compos Sci Technol* 69(13), 2009, pp. 2163–2168.

[114] Y. Z. Wan, H. Luo, F. He, H. Liang, Y. Huang, and X. L. Li. "Mechanical, moisture absorption, and biodegradation behaviours of bacterial cellulose fibre-reinforced starch biocomposites". *Compos Sci Technol* 69(7–8), 2009, pp. 1212–1217.

[115] C. J. Grande, F. G. Torres, C. M. Gomez, and M. Carmen Bañó. "Nanocomposites of bacterial cellulose/hydroxyapatite for biomedical applications". *Acta Biomater* 5(5), 2009, pp. 1605–1615.

[116] T. Nishino, I. Matsuda, and K. Hirao. "All-Cellulose Composite". *Macromolecules* 37(20), 2004, pp. 7683–7687.

[117] N. Soykeabkaew, C. Sian, S. Gea, T. Nishino, and T. Peijs. "All-cellulose nanocomposites by surface selective dissolution of bacterial". *Cellulose* 16(3), 2009, pp. 435–444.

[118] *High Performance Carbon Fibers - National Historic Chemical Landmark*. 2003. URL: `http://www.acs.org/content/acs/en/education/whatischemistry/landmarks/carbonfibers.html` (visited on 02/21/2014).

[119] R. Bacon. “Growth, Structure, and Properties of Graphite Whiskers”. *J Appl Phys* 31(2), 1960, pp. 283–290.

[120] A. Shindo. “Report of the Government Industrial Research Institute”. *Osaka.(317)* 1961.

[121] A. Shindo. “Studies on graphite fiber”. *J. Ceram. Assoc. Japan* 69, 1961, p. C195.

[122] N. R. C. (C. o. H.-P. S. F. f. Composites. *High-performance synthetic fibers for composites: report of the Committee on High-Performance Synthetic Fibers for Composites*. 1992.

[123] L. S. Singer. “The mesophase and high modulus carbon fibers from pitch”. *Carbon* 16(6), 1978, pp. 409–415.

[124] “High modulus, high strength carbon fibers produced from mesophase pitch”. US4005183 A. L. S. Singer. 1977.

[125] S. Chand. “Review Carbon fibers for composites”. *J Mater Sci* 35(6), 2000, pp. 1303–1313.

[126] Engineering news online. *Airbus to start manufacturing parts for new A350 XWB in late ’09*. 2009. URL: `http://www.engineeringnews.co.za/article/airbus-to-start-manufacturing-parts-for-new-a350-xwb-in-late-09-2009-05-11` (visited on 12/04/2011).

[127] John Croft. “Airbus and Boeing spar for middleweight title”. *Aerospace Am* 43(7), 2005, pp. 36–42.

[128] Boeing. *Boeing 787 Dreamliner will provide new solutions for airlines, passengers*. Boeing: Commercial Airplanes - 787 Dreamliner - Background. URL: `http://www.boeing.com/commercial/787family/background.html` (visited on 12/04/2011).

[129] *MarketsandMarkets: Global Carbon Fiber (CF) Production to Reach 80,000 Tons in 2016; US and Japan to Remain Largest Carbon Fiber Supply Regions, Forecasts Report*. 2013. URL: `http://www.marketsandmarkets.com/PressReleases/carbon-fiber.asp` (visited on 02/21/2014).

[130] F. S. Baker. “Low cost carbon fiber from renewable resources”. *EERE, US Dept of Energy Project ID# lm_03_baker* 2010.

[131] A. L. Compere, W. L. Griffith, C. F. Leitten, and J. T. Shaffer. “Low cost carbon fiber from renewable resources”. *International SAMPE Technical Conference*. Vol. 33. 2001, pp. 1306–1314.

[132] A. G. Dumanlı and A. H. Windle. “Carbon fibres from cellulosic precursors: a review”. *J Mater Sci* 47(10), 2012, pp. 4236–4250.

[133] X. Huang. “Fabrication and Properties of Carbon Fibers”. *Mater Res Soc Symp P* 2(4), 2009, pp. 2369–2403.

[134] R. E. Franklin. “Crystallite Growth in Graphitizing and Non-Graphitizing Carbons”. *Proceedings of the Royal Society of London. Series A. Mathematical and Physical Sciences* 209(1097), 1951, pp. 196–218.

[135] J. J. Kipling, J. N. Sherwood, P. V. Shooter, and N. R. Thompson. “Factors influencing the graphitization of polymer carbons”. *Carbon* 1(3), 1964, pp. 315–320.

[136] I. Mochida, Y. Korai, C.-H. Ku, F. Watanabe, and Y. Sakai. "Chemistry of synthesis, structure, preparation and application of aromatic-derived mesophase pitch". *Carbon* 38(2), 2000, pp. 305–328.

[137] *Pitch-based Carbon Fiber(CF) - Industrial Materials | Mitsubishi Plastics, Inc.* 2012. URL: `https://www.mpi.co.jp/english/products/industrial%5C_materials/pitch%5C_based%5C_carbon%5C_fiber/pbcf001.html` (visited on 03/04/2014).

[138] J. Donnet. *Carbon fibers*. CRC, 1998.

[139] *Toray Insustries, Inc. TORAYCA*. 2005. URL: `http://www.torayca.com/en/index.html` (visited on 03/04/2014).

[140] O. Ishida, D.-Y. Kim, S. Kuga, Y. Nishiyama, and R. M. B. Jr. "Microfibrillar carbon from native cellulose". *Cellulose* 11(3), 2004, pp. 475–480.

[141] D. J. Johnson. "Structure-property relationships in carbon fibres". *J. Phys. D: Appl. Phys.* 20(3), 1987, p. 286.

[142] G. Henrici-Olivé and S. Olivé. "The chemistry of carbon fiber formation from polyacrylonitrile". *Industrial Developments*. Advances in Polymer Science 51. Springer Berlin Heidelberg, 1983, pp. 1–60.

[143] D. Edie. "The effect of processing on the structure and properties of carbon fibers". *Carbon* 36(4), 1998, pp. 345–362.

[144] M. Rahaman, A. Ismail, and A. Mustafa. "A review of heat treatment on polyacrylonitrile fiber". *Polym Degrad Stabil* 92(8), 2007, pp. 1421–1432.

[145] K. B. Wiles. "Determination of Reactivity Ratios for Acrylonitrile/Methyl Acrylate Radical Copolymerization Via Nonlinear Methodologies Using Real Time FTIR". Master's Thesis. Virginia Polytechnic Institute and State University, 2002.

[146] B. J. Wicks and R. A. Coyle. "Microstructural inhomogeneity in carbon fibres". *J Mater Sci* 11(2), 1976, pp. 376–383.

[147] R. J. Diefendorf and E. Tokarsky. "High-performance carbon fibers". *Polymer Engineering & Science* 15(3), 1975, pp. 150–159.

[148] R. H. Knibbs. "The use of polarized light microscopy in examining the structure of carbon fibres∗". *J. Microsc.* 94(3), 1971, pp. 273–281.

[149] M. Minus and S. Kumar. "The processing, properties, and structure of carbon fibers". *Jom-us* 57(2), 2005, pp. 52–58.

[150] F. Smith, T. Eckle, R. Osterholm, and R. Stichel. *Manufacture of coal tar and pitches. Bituminous Materials. Asphalts, tars and pitches*. Ed. by A. J. Hoiberg. Vol. 3. InterScience Publishers: New York, NY, USA, 1966, p. 57.

[151] J. Brooks and G. Taylor. "The formation of graphitizing carbons from the liquid phase". *Carbon* 3(2), 1965, pp. 185–193.

[152] T. Matsumoto. "Mesophase pitch and its carbon fibers". *Pure & Appl. Chem* 57(11), 1985, pp. 1553–1562.

[153] D. Chung. *Carbon fiber composites*. Boston, MA: Butterworth-Heinemann, 1994, pp. 3–65.

[154] A. A. Bright and L. S. Singer. "The electronic and structural characteristics of carbon fibers from mesophase pitch". *Carbon* 17(1), 1979, pp. 59–69.

[155] G. M. W. M. Reed Haddock and R. V. Cook. *NARC rayon replacement program for the RSRM nozzle, phase IV qualification and implementation status*. American Institute of Aeronautics and Astronautics, 2005.

[156] R. C. Rossi and W. C. Wong. *Availability of aerospace rayon for SRM nozzle insulators*. American Institute of Aeronautics and Astronautics, 1995.

[157] G. B. Kauffman. "Rayon: The first semi-synthetic fiber product". *J Chem Educ* 70(11), 1993, p. 887.

[158] M. Tang and R. Bacon. "Carbonization of cellulose fibers—I. Low temperature pyrolysis". *Carbon* 2(3), 1964, pp. 211–220.

[159] "Process for producing carbon fibers having a high young's modulus of elasticity". 3716331. W. A. Schalamon and R. Bacon. 1973.

[160] W. Ruland. "X-Ray Studies on Preferred Orientation in Carbon Fibers". *Journal of Applied Physics* 38(9), 1967, p. 3585.

[161] H. Chanzy, A. Peguy, S. Chaunis, and P. Monzie. "Oriented cellulose films and fibers from a mesophase system". *Journal of Polymer Science: Polymer Physics Edition* 18(5), 1980, pp. 1137–1144.

[162] C. C. McCorsley III. "Process for shaped cellulose article prepared from a solution containing cellulose dissolved in a tertiary amine N-oxide solvent". US Patent 4,246,221. 1981.

[163] H. Boerstoel, H. Maatman, J. Westerink, and B. Koenders. "Liquid crystalline solutions of cellulose in phosphoric acid". *Polymer* 42(17), 2001, pp. 7371–7379.

[164] H. Coulsey and S. Smith. "The formation and structure of a new cellulosic fibre". *Lenzinger Berichte* 75, 1996, pp. 51–61.

[165] M. Northolt, H. Boerstoel, H. Maatman, R. Huisman, J. Veurink, and H. Elzerman. "The structure and properties of cellulose fibres spun from an anisotropic phosphoric acid solution". *Polymer* 42(19), 2001, pp. 8249–8264.

[166] S. Peng, H. Shao, and X. Hu. "Lyocell fibers as the precursor of carbon fibers". *Journal of applied polymer science* 90(7), 2003, pp. 1941–1947.

[167] K. Kong, L. Deng, I. A. Kinloch, R. J. Young, and S. J. Eichhorn. "Production of carbon fibres from a pyrolysed and graphitised liquid crystalline cellulose fibre precursor". *J Mater Sci* 47(14), 2012, pp. 5402–5410.

[168] Y. Kaburagi, K. Hosoya, A. Yoshida, and Y. Hishiyama. "Thin graphite skin on glass-like carbon fiber prepared at high temperature from cellulose fiber". *Carbon* 43(13), 2005, pp. 2817–2819.

[169] X. Zhang, Y. Lu, H. Xiao, and H. Peterlik. "Effect of hot stretching graphitization on the structure and mechanical properties of rayon-based carbon fibers". *Journal of Materials Science* 49(2), 2014, pp. 673–684.

[170] D. Li, H. Wang, and X. Wang. "Effect of microstructure on the modulus of PAN-based carbon fibers during high temperature treatment and hot stretching graphitization". *Journal of materials science* 42(12), 2007, pp. 4642–4649.

[171] D.-Y. Kim, Y. Nishiyama, M. Wada, and S. Kuga. "Graphitization of highly crystalline cellulose". *Carbon* 39(7), 2001, pp. 1051–1056.

[172] H. Sakata, G. Dresselhaus, M. S. Dresselhaus, and M. Endo. "Effect of uniaxial stress on the Raman spectra of graphite fibers". *J Appl Phys* 63(8), 1988, p. 2769.

[173] M. Endo. "Structure of mesophase pitch-based carbon fibres". *J Mater Sci* 23(2), 1988, pp. 598–605.

[174] H. P. Klug and L. E. Alexander. "X-ray diffraction procedures: for polycrystalline and amorphous materials". *X-Ray Diffraction Procedures: For Polycrystalline and Amorphous Materials, 2nd Edition, by Harold P. Klug, Leroy E. Alexander, pp. 992. ISBN 0-471-49369-4. Wiley-VCH, May 1974.* 1, 1974.

[175] F. Liu, H. Wang, L. Xue, L. Fan, and Z. Zhu. "Effect of microstructure on the mechanical properties of PAN-based carbon fibers during high-temperature graphitization". *J Mater Sci* 43(12), 2008, pp. 4316–4322.

[176] F. Tuinstra and J. L. Koenig. "Raman spectrum of graphite". *The Journal of Chemical Physics* 53(3), 2003, pp. 1126–1130.

[177] G. A. Zickler, B. Smarsly, N. Gierlinger, H. Peterlik, and O. Paris. "A reconsideration of the relationship between the crystallite size L_a of carbons determined by X-ray diffraction and Raman spectroscopy". *Carbon* 44(15), 2006, pp. 3239–3246.

[178] M. Roman and W. T. Winter. "Effect of sulfate groups from sulfuric acid hydrolysis on the thermal degradation behavior of bacterial cellulose". *Biomacromolecules* 5(5), 2004, pp. 1671–1677.

[179] D.-Y. Kim, Y. Nishiyama, M. Wada, and S. Kuga. "High-yield carbonization of cellulose by sulfuric acid impregnation". *Cellulose* 8(1), 2001, pp. 29–33.

[180] F. Zeng, D. Pan, and N. Pan. "Choosing the Impregnants by Thermogravimetric Analysis for Preparing Rayon-Based Carbon Fibers". *J Inorg Organomet P* 15(2), 2005, pp. 261–267.

[181] Z. L. Wang and W. Wu. "Nanotechnology-Enabled Energy Harvesting for Self-Powered Micro-/Nanosystems". *Angewandte Chemie International Edition* 51(47), 2012, pp. 11700–11721.

[182] C. J. Brabec. "Organic photovoltaics: technology and market". *Solar energy materials and solar cells* 83(2), 2004, pp. 273–292.

[183] M. A. Green. *Third generation photovoltaics: advanced solar energy conversion*. Vol. 12. Springer, 2006.

[184] *Photovoltaics*. Office of Energy Efficiency & Renewable Energy. 2014. URL: `http://energy.gov/eere/sunshot/photovoltaics` (visited on 05/30/2014).

[185] D. Mills. "Advances in solar thermal electricity technology". *solar Energy* 76(1), 2004, pp. 19–31.

[186] S. A. Kalogirou. "Solar thermal collectors and applications". *Progress in energy and combustion science* 30(3), 2004, pp. 231–295.

[187] M. R. Spangler and G. Bredehoeft. *2013 completions of large solar thermal power plants mark technology gains*. U.S. Energy Information Administration. 2013. URL: `http://www.eia.gov/todayinenergy/detail.cfm?id=13791` (visited on 05/30/2014).

[188] M. Liserre, R. Cardenas, M. Molinas, and J. Rodriguez. "Overview of multi-MW wind turbines and wind parks". *Industrial Electronics, IEEE Transactions on* 58(4), 2011, pp. 1081–1095.

[189] A. Bridgwater. "The technical and economic feasibility of biomass gasification for power generation". *Fuel* 74(5), 1995, pp. 631–653.

[190] *Siemens wins 1.5-billion-euro wind park contract to supply wind turbines*. The Economic Times. 2014. URL: `http://articles.economictimes.indiatimes.com/2014-05-15/news/49873594_1_wind-turbines-wind-power-plant-gemini` (visited on 05/30/2014).

[191] Z. Haq. *Biomass for electricity generation*. U.S. Energy Information Administration. 2002. URL: `http://www.eia.gov/oiaf/analysispaper/biomass/` (visited on 05/30/2014).

[192] "Tidal/Wave Energy". *Fuel and Energy Abstracts*. 1996, p. 443.

[193] M. E. McCormick. *Ocean wave energy conversion*. Courier Dover Publications, 2013.

[194] M. S. Dresselhaus, G. Chen, M. Y. Tang, R. Yang, H. Lee, D. Wang, Z. Ren, J.-P. Fleurial, and P. Gogna. "New Directions for Low-Dimensional Thermoelectric Materials". *Advanced Materials* 19(8), 2007, pp. 1043–1053.

[195] A. Minnich, M. Dresselhaus, Z. Ren, and G. Chen. "Bulk nanostructured thermoelectric materials: current research and future prospects". *Energy & Environmental Science* 2(5), 2009, pp. 466–479.

[196] B. E. Logan, B. Hamelers, R. Rozendal, U. Schröder, J. Keller, S. Freguia, P. Aelterman, W. Verstraete, and K. Rabaey. "Microbial fuel cells: methodology and technology". *Environmental science & technology* 40(17), 2006, pp. 5181–5192.

[197] A. Deeke, T. H. J. A. Sleutels, H. V. M. Hamelers, and C. J. N. Buisman. "Capacitive Bioanodes Enable Renewable Energy Storage in Microbial Fuel Cells". *Environmental Science & Technology* 46(6), 2012, pp. 3554–3560.

[198] D. P. B. T. B. Strik, H. V. M. Hamelers (Bert), J. F. H. Snel, and C. J. N. Buisman. "Green electricity production with living plants and bacteria in a fuel cell". *Int J Energ Res* 32(9), 2008, pp. 870–876.

[199] A. Navid and L. Pilon. "Pyroelectric energy harvesting using Olsen cycles in purified and porous poly (vinylidene fluoride-trifluoroethylene)[P (VDF-TrFE)] thin films". *Smart Materials and Structures* 20(2), 2011, p. 025012.

[200] F. Y. Lee, S. Goljahi, I. M. McKinley, C. S. Lynch, and L. Pilon. "Pyroelectric waste heat energy harvesting using relaxor ferroelectric 8/65/35 PLZT and the Olsen cycle". *Smart Materials and Structures* 21(2), 2012, p. 025021.

[201] Mark Gregory. *Energy harvesting: lighting the office - by walking.* 2013. URL: http://www.bbc.co.uk/news/business-23281950 (visited on 2014).

[202] A. Abbasi. "Application of Piezoelectric Materials and Piezoelectric Network for Smart Roads". *International Journal of Electrical and Computer Engineering (IJECE)* 3(6), 2013, pp. 857–862.

[203] F.-R. Fan, Z.-Q. Tian, and Z. Lin Wang. "Flexible triboelectric generator". *Nano Energy* 1(2), 2012, pp. 328–334.

[204] G. Zhu, Z.-H. Lin, Q. Jing, P. Bai, C. Pan, Y. Yang, Y. Zhou, and Z. L. Wang. "Toward large-scale energy harvesting by a nanoparticle-enhanced triboelectric nanogenerator". *Nano letters* 13(2), 2013, pp. 847–853.

[205] S. Roundy, E. S. Leland, J. Baker, E. Carleton, E. Reilly, E. Lai, B. Otis, J. M. Rabaey, P. K. Wright, and V. Sundararajan. "Improving power output for vibration-based energy scavengers". *Pervasive Computing, IEEE* 4(1), 2005, pp. 28–36.

[206] Y. K. Ramadass and A. P. Chandrakasan. "A Battery-Less Thermoelectric Energy Harvesting Interface Circuit With 35 mV Startup Voltage". *Ieee J Solid-st Circ* 46(1), 2011, pp. 333–341.

[207] L. M. Tender, S. A. Gray, E. Groveman, D. A. Lowy, P. Kauffman, J. Melhado, R. C. Tyce, D. Flynn, R. Petrecca, and J. Dobarro. "The first demonstration of a microbial fuel cell as a viable power supply: Powering a meteorological buoy". *J Power Sources* 179(2), 2008, pp. 571–575.

[208] Z. L. Wang. "Piezoelectric Nanogenerators Based on Zinc Oxide Nanowire Arrays". *Int S Techn Pol Inn* 312(5771), 2006, pp. 242–246.

[209] G. Zhu, R. Yang, S. Wang, and Z. L. Wang. "Flexible High-Output Nanogenerator Based on Lateral ZnO Nanowire Array". *Nano Lett* 10(8), 2010, pp. 3151–3155.

[210] W. W. Wolny. "European approach to development of new environmentally sustainable electroceramics". *Ceramics international* 30(7), 2004, pp. 1079–1083.

[211] E. Fukada. "Piezoelectricity of Wood". *J Phys Soc Jpn* 10(2), 1955, pp. 149–154.

[212] V. Bazhenov and V. Konstantinova. "Piezoelectric effect of wood". *Doklady Academy Nauk SSSR*. Vol. 71. 1950, pp. 283–286.

[213] E. Fukada. "Piezoelectricity as a fundamental property of wood". *Wood Sci Technol* 2(4), 1968, pp. 299–307.

[214] W. Cady. *Piezoelectricity. 1946.* McGraw-Hill, New York, 1947.

[215] A. Safari and E. K. Akdogan. *Piezoelectric and acoustic materials for transducer applications.* Springer, 2008.

[216] P. Hermans. "X-ray investigations on the crystallinity of cellulose". *Die Makromolekulare Chemie* 6(1), 1951, pp. 25–29.

[217] E. Fukada. "History and recent progress in piezoelectric polymers". *Ultrasonics, Ferroelectrics and Frequency Control, IEEE Transactions on* 47(6), 2000, pp. 1277–1290.

[218] N. Hirai, N. Sobue, and I. Asano. “Studies on piezoelectric effect of wood. IV. Effects of heat treatment on cellulose crystallites and piezoelectric effect of wood”. *Jap Wood Res Soc J* 1972.

[219] N. Hirai and A. Yamaguchi. “Studies on piezoelectric effect of wood. VII. Effect of moisture content on piezoelectric dispersion of wood”. *Mokuzai Gakkaishi* 25(1), 1979, pp. 1–6.

[220] J. Kim, S. Yun, and Z. Ounaies. “Discovery of Cellulose as a Smart Material”. *Macromolecules* 39(12), 2006, pp. 4202–4206.

[221] J. Kim, C.-S. Song, and S.-R. Yun. “Cellulose based electro-active papers: performance and environmental effects”. *Vtt Symp* 15(3), 2006, pp. 719–723.

[222] H. S. Kim, Y. Li, and J. Kim. “Electro-mechanical behavior and direct piezoelectricity of cellulose electro-active paper”. *Sensors and Actuators A: Physical* 147(1), 2008, pp. 304–309.

[223] W. Cousins. “Young’s modulus of hemicellulose as related to moisture content”. *Wood science and technology* 12(3), 1978, pp. 161–167.

[224] S. Yun, J. Kim, and C. Song. “Performance of Electro-active paper actuators with thickness variation”. *Sensors and Actuators A: Physical* 133(1), 2007, pp. 225–230.

[225] S. Yun and J. Kim. “A bending electro-active paper actuator made by mixing multi-walled carbon nanotubes and cellulose”. *Vtt Symp* 16(4), 2007, pp. 1471–1476.

[226] S. K. Mahadeva, K. Walus, and B. Stoeber. “Piezoelectric Paper Fabricated via Nanostructured Barium titanate Functionalization of Wood Cellulose Fibers”. *ACS applied materials & interfaces* 2014.

[227] S.-S. Kim, J.-H. Jeon, C.-D. Kee, and I.-K. Oh. “Electro-active hybrid actuators based on freeze-dried bacterial cellulose and PEDOT: PSS”. *Smart Materials and Structures* 22(8), 2013, p. 085026.

[228] K. O-Rak, S. Ummartyotin, M. Sain, and H. Manuspiya. “Covalently grafted carbon nanotube on bacterial cellulose composite for flexible touch screen application”. *Materials Letters* 107, 2013, pp. 247–250.

[229] J.-H. Jeon, I.-K. Oh, C.-D. Kee, and S.-J. Kim. “Bacterial cellulose actuator with electrically driven bending deformation in hydrated condition”. *Sensors and Actuators B: Chemical* 146(1), 2010, pp. 307–313.

[230] L. Zhai, B.-W. Kang, J.-H. Kim, J. Kim, Z. Abas, and H. S. Kim. “Electrode effect on the cellulose piezo-paper energy harvester”. *SPIE Smart Structures and Materials+ Nondestructive Evaluation and Health Monitoring*. International Society for Optics and Photonics. 2013, 86870R–86870R.

[231] J. Kim and Y. B. Seo. “Electro-active paper actuators”. *Vtt Symp* 11(3), 2002, pp. 355–360.

[232] J. Kim, S.-H. Bae, and H.-G. Lim. “Micro transfer printing on cellulose electro-active paper”. *Vtt Symp* 15(3), 2006, pp. 889–892.

[233] I. Kuehne, D. Marinkovic, G. Eckstein, and H. Seidel. “A new approach for MEMS power generation based on a piezoelectric diaphragm”. *Sensors and Actuators A: Physical* 142(1), 2008, pp. 292–297.

[234] E. Hong, S. Trolier-McKinstry, R. L. Smith, S. V. Krishnaswamy, and C. B. Freidhoff. "Design of MEMS PZT circular diaphragm actuators to generate large deflections". *Microelectromechanical Systems, Journal of* 15(4), 2006, pp. 832–839.